AD_____

AWARD NUMBER DAMD17-98-1-8338

TITLE: Inhibition of Breast Cancer Metastasis by Heregulin-Beta 1

PRINCIPAL INVESTIGATOR: Dihua Yu, M.D., Ph.D.

CONTRACTING ORGANIZATION: The University of Texas
Houston, Texas 77030

REPORT DATE: June 1999

TYPE OF REPORT: Annual

PREPARED FOR: U.S. Army Medical Research and Materiel Command
Fort Detrick, Maryland 21702-5012

REPORT DOCUMENTATION PAGE

Form Approved
OMB No. 0704-0188

1. AGENCY USE ONLY *(Leave blank)*	2. REPORT DATE	3. REPORT TYPE AND DATES COVERED
	June 1999	Annual (1 Jun 98 - 31 May 99)

4. TITLE AND SUBTITLE
Inhibition of Breast Cancer Metastasis by Heregulin-Beta 1

5. FUNDING NUMBERS
DAMD17-98-1-8338

6. AUTHOR(S)
Dihua Yu, M.D., Ph.D.

7. PERFORMING ORGANIZATION NAME(S) AND ADDRESS(ES)
The University of Texas
Houston, Texas 77030

8. PERFORMING ORGANIZATION REPORT NUMBER

9. SPONSORING / MONITORING AGENCY NAME(S) AND ADDRESS(ES)
U.S. Army Medical Research and Materiel Command
Fort Detrick, Maryland 21702-5012

10. SPONSORING / MONITORING AGENCY REPORT NUMBER

11. SUPPLEMENTARY NOTES

12a. DISTRIBUTION / AVAILABILITY STATEMENT
Approved for public release; distribution unlimited

12b. DISTRIBUTION CODE

13. ABSTRACT *(Maximum 200 words)*

The major goal of this Idea proposal is to determine whether and how HRG-β1 inhibits breast cancer metastasis and to identify the functional domains that are sufficient for inhibition of breast cancer metastasis. We have fulfilled most of the proposed tasks for the first year of the grant support. We demonstrated that the recombinant HRG-β1 can transcriptionally upregulate gelatinases activity. We found that HRG-β1 induces the aggregation (a metastasis associated property) of breast cancer cells via activation of PI-3-K but independent of ERK (*Cancer Res.* 59: 1620-1625, 1999). To determine the effect of HRG-β1 in metastasis *in vivo*, we subcloned the extracellular domain of the full length HRG-β1 into the pSecTag2 expression vector, transfected it into MDA-MB-435 and MCF-7 cell, and established stable transfectants. To further delineate the domain(s) of HRG-β1 that regulates invasion/metastasis of breast cancer cells, we have also cloned the egf-like domain of HRG-β1 to pSecTag2 expression vector. We are transfecting the egf-like domain of HRG-β1 into MDA-MB-435 and MCF-7 cells to establish stable transfectants. These initial works have paved a productive avenue for the next grant-support year, when we will gain more insights regarding the role of HRG-β1 in breast cancer metastasis.

14. SUBJECT TERMS
Breast Cancer, Heregulin, metastasis, invasion, transfectants, mutants

15. NUMBER OF PAGES
38

16. PRICE CODE

17. SECURITY CLASSIFICATION OF REPORT	18. SECURITY CLASSIFICATION OF THIS PAGE	19. SECURITY CLASSIFICATION OF ABSTRACT	20. LIMITATION OF ABSTRACT
Unclassified	Unclassified	Unclassified	Unlimited

FOREWORD

Opinions, interpretations, conclusions and recommendations are those of the author and are not necessarily endorsed by the U.S. Army.

____ Where copyrighted material is quoted, permission has been obtained to use such material.

____ Where material from documents designated for limited distribution is quoted, permission has been obtained to use the material.

____ Citations of commercial organizations and trade names in this report do not constitute an official Department of Army endorsement or approval of the products or services of these organizations.

__✓__ In conducting research using animals, the investigator(s) adhered to the "Guide for the Care and Use of Laboratory Animals," prepared by the Committee on Care and use of Laboratory Animals of the Institute of Laboratory Resources, national Research Council (NIH Publication No. 86-23, Revised 1985).

__✓__ For the protection of human subjects, the investigator(s) adhered to policies of applicable Federal Law 45 CFR 46.

__✓__ In conducting research utilizing recombinant DNA technology, the investigator(s) adhered to current guidelines promulgated by the National Institutes of Health.

__✓__ In the conduct of research utilizing recombinant DNA, the investigator(s) adhered to the NIH Guidelines for Research Involving Recombinant DNA Molecules.

____ In the conduct of research involving hazardous organisms, the investigator(s) adhered to the CDC-NIH Guide for Biosafety in Microbiological and Biomedical Laboratories.

PI - Signature 6-21-99 Date

TABLE OF CONTENTS

Introduction

Breast cancer is one of the most common malignancies among women in the United States, and metastasis is the major cause of death for breast cancer patients. Therefore, it is extremely important to uncover the basis of breast cancer metastasis. Studies from our laboratory demonstrated that overexpression of the *erb*B2 gene (also known as HER-2/*neu*), which encodes a receptor tyrosine kinase that belongs to the epidermal growth factor receptor subfamily, enhances intrinsic metastatic potential in human breast cancer cells without increasing their transformation abilities. As we were pursuing the molecular mechanisms underlying *erb*B2-induced metastasis, we unexpectedly discovered that human heregulin-β1 (HRG-β1), which is a ligand for the erbB3- and erbB4-encoded growth factor receptors and can activate erbB2 by inducing heterodimerization between erbB2 and erbB3 or erbB4, can inhibit some invasion/metastasis-associated properties in MDA-MB-435 breast cancer cells. This unexpected finding led us to hypothesize that HRG-β1 inhibits breast cancer metastasis through specific functional domains. The major goal of research supported by this Idea grant is to determine whether and how HRG-β1 inhibits breast cancer metastasis and to identify the specific structural motifs or functional domains that are sufficient for inhibition of breast cancer metastasis. We have proposed three Specific Aims to fulfill our major goal. During the first funding year, we have performed our studies on parts of all three Specific Aims (see below). We believe that The initial research progress have paved a productive avenue for the next grant-support year, when we will gain more insights regarding the role of HRG-β1 in breast cancer metastasis.

Body

During the first funding year, we have performed our studies on parts of all three Specific Aims, including the following tasks:

Objective 1. To further determine the inhibitory effect of HRG-β1 on invasion/metastasis-associated properties

Task 1: Months 1-8 (student 1): Investigate the effects of HRG-β1 on the secretion of basement membrane/ECM-degrading enzymes by MDA-MB-435 breast cancer cells.

To test whether HRG-β1 can modulate MMP-9 (gelatinase) activation in MDA-MB-435 human breast cancer cells, we treated the MDA-MB-435 breast cancer cell line with or without recombinant HRG-β1 for 24 hrs. We then collected conditioned media from the treated or untreated cells and performed zymogram analysis on MMP-9 activity. As shown in Fig.1A below, HRG treatment did not alter the MMP-9 activities in MDA-MB-435 cells. To make sure the recombinant HRG-β1 we used was functional, and to also test the effect of HRG-β1on other breast cancer cell lines, we treated a panel of breast cancer cell lines with or without recombinant HRG-β1. We then collected conditioned media from these cells and did zymogram analysis of MMP-9 activity. HRG-β1 treatment led to dramatic increase in MMP-9 activities in MCF-7

and SKBR3 cells (i.e., the recombinant HRG-β1 is functional) but not in BT474 cells (Fig. 1A, Appendix A, all figures are in Appendix A), nor in MDA-MB-231 cells (data not shown). These suggest that HRG-β1 did not inhibit MMP-9 activity in MDA-MB-435 cells, and HRG-β1 modulates MMP-9 activities in a cell line-dependent manner. Since MCF-7 and SKBR3 cells express higher levels of the erbB3 receptor of HRG than MDA-MB-435, BT 474, and MDA-MB-231 cells, HRG-β1 modulation of MMP-9 activities may only be significant in breast cancer cells that express high levels of erbB3 or erbB4 receptors. Moreover, the induction of MMP-9 activity by HRG-β1 in MCF-7 and SKBR3 cells was both dose and time dependent (Fig.1B).

Although upregulation of MMP-9 by HRG-β1 in SKBR3 cells has been reported, the molecular mechanisms were unknown. Although this question was not proposed in the original proposal, it is a related and very important issue. We therefore further examined whether HRG-β1 stimulation increased mRNA levels of MMP-9 in SKBR3 cells. As shown in Fig.2, basal mRNA level of MMP-9 in SKBR3 cells is very low. Increase in mRNA level of MMP-9 can be detected as early as six hours after HRG treatment. The level of MMP-9 mRNA continued to increase 24 hr after stimulation. This result suggested that the transcription of MMP-9 gene may be upregulated after HRG-β1 treatment. To determine whether transcription of MMP-9 is upregulated by HRG-β1, we constructed a series of MMP-9 promoter deletion constructs fused with luciferase reporter gene. We transfected these reporter genes to SKBR3 cells treated with or without HRG-β1, and measured the promoter activities by luciferase assays. We found that the luciferase activity can be upregulated by HRG-β1 treatment (Fig. 3). These data suggest that transcription of MMP-9 is indeed upregulated by HRG-β1. Furthermore, we identified the HRG-β1–responding element in the MMP9 promoter (-84 to –241). Currently, we are investigating the transcription factors and signaling pathways that leads to this transcription upregulation of MMP-9 by HRG-β. We expect to write a manuscript on these studies in the second funding year.

Note: The above-described works have taken student 1 about 8 months. This explains why we have task 2 unfinished, and we plan to accomplish it in the second funding year.

Task 3: Months 1-6 (student 2): Determine whether HRG-β1 may inhibit invasion and invasion/ metastasis-associated properties in other breast cancer cell lines.

We reported in our original proposal that HRG-β1 inhibited invasion of MDA-MB-435 breast cancer cells. To further investigate whether inhibition of invasion by HRG-β1 is a general effect for breast cancer cells, we also examined the invasion-inhibitory effect of HRG-β1 on other human breast cancer cell lines that have been shown to induce metastatic tumors in nude or SCID mice, including MCF-7; MDA-MB-231 [Zhang, 1991 #747] and SKBR3 cells. HRG-β1 inhibited invasion of MDA-MB-231 cells but enhanced invasion of MCF-7 and SK-BR-3 cells (Fig. 4). The discrepant effects of HRG-β1 on invasion between MDA-MB-435, MDA-MB-231 and the MCF-7, SKBR-3 cell lines are likely due to their different genetic backgrounds, especially, erbB3 and erbB4 receptor levels. As described above, we have also examined these breast cancer cell lines for proteases activities and found that HRG-β1

also had different effects on protease activities on these different cell lines. In addition, tumor cell homophilic adhesion may negatively affect invasive and metastatic potential of cells. We have tested the effects of HRG-β1 on aggregation of MDA-MB-435, MDA-MB-231, MCF-7, and SKBR3 human breast cancer cells. We found that HRG-β1 enhances aggregation of all these cells (Appendix B, *Cancer Res.* 59: 1620-1625, 1999). This raise the possibility that for erbB3 high expressing cell, such as MCF-7 and SKBR3, HRG-β1 may have impacts on certain invasion/metastasis-associated properties that promotes metastasis (e.g., invasion, protease secretion), but may also have impacts on other invasion/metastasis-associated properties that inhibit metastasis (e.g. aggregation). Whereas for erbB3 low expressing cells such as MDA-MB-435 and MDA-MB-231 cells, HRG-β1 mainly have effects on certain invasion/metastasis-associated properties that inhibit metastasis but no effect on other invasion/metastasis-associated properties that enhance metastasis (e.g., protease secretion). To determine the effect of HRG-β1 on metastasis, the ultimate test would be *in vivo* metastasis assays that require the establishment of HRG-β1 transfectants (see below).

Although not proposed in the original proposal, we believe it is critical to investigate the downstream signals involved in HRG-β1-enhaced cell aggregation. We observed that HRG-β1 induced tyrosine phosphorylation of erbB2 and erbB3 receptor heterodimers and increased the association of the dimerized receptors with the 85-KDa subunit of phosphatidylinositol 3-kinase (PI3K). HRG-β1 also increased the kinase activities of extracellular signal-regulated protein kinase (ERK) and PI3K in these cells. By using the MAPK/ERK kinase 1 (MEK1) inhibitor PD98059 and PI3K inhibitors wortmannin and LY294002, we found that blocking the MEK1-ERK pathway had no effect on HRG-β1-enhanced cell aggregation; however, blocking the PI3K pathway greatly inhibited HRG-β1-mediated cell aggregation. Our study indicated that the HRG-β1-activated MEK1-ERK pathway has no demonstrable role in the induction of cell aggregation, whereas HRG-β1-activated PI3K is required for enhancing breast cancer cell aggregation. Our results have provided one mechanism by which HRG-β1-activated signaling of erbB receptors may affect invasive/metastatic properties of breast cancer cells (Appendix B, *Cancer Res.* 59: 1620-1625, 1999).

Note: The above-described works have taken student 2 (with some help from student 1) more than a year to get paper published. This explains why we have tasks 8 and 9 partially done, and we plan to accomplish more in the second funding year.

Objective 2. To test whether HRG-β1 may inhibit breast cancer metastasis *in vivo*

Task 4: Months 7-12 (student 1):): Subcloning of HRG-β1 full extracellular domain into pSecTag2 expression vector. Transfection of this expression vector into the MDA-MB-435 cells and establish stable transfectants.

The ultimate test for determining the effects of HRG-β1 on metastasis is *in vivo* metastasis assays that require the establishment of HRG-β1 transfectants. In the original proposal, we only proposed to transfect the HRG-β1 expression vector into the MDA-MB-435 cells and establish stable transfectants. To determine the effects of HRG-β1 on both erbB3 low and high expressing breast cancer cells, we have taken additional efforts to also establish HRG-β1 stable transfectants in MCF-7 cells. We first confirmed that both cell lines do express the erbB3 receptors (Fig. 5A) but not express HRG in conditioned medium (Fig 5B) or total cell extract (data not shown). The differences in erbB3 expression level between MDA-MB-435 and MCF-7 cell lines will allow us to examine the effects of HRG-β1 on both erbB3 low (MDA-MB-435) and high (MCF-7) expressing breast cancer cells. Although the receptor erbB4 binds HRG, it binds with lower affinity

than erbB3 and erbB4 is expressed at similar levels in both cell lines (data not shown). In order to study the *in vivo* effects of heregulin-β1 on metastasis, we subcloned the full extracellular domain of HRG-β1 into the pSecTag2 secretion vector that contained histidine and myc tags for easy detection (Fig. 6). The HRG-β1 constructs and the vector control (zeocin resistance) were transfected into MDA-MB 435 and MCF-7 cells. Drug selection (zeocin resistance) was used to obtain two or more high expressing clones that were identified at their estimated molecular weights by anti-HRG or anti-histidine antibodies using western blot analysis (Figs. 7 and 8). Next, we determined whether the stable transfectants secreted full extracellular domain HRG proteins that have biological functions. The ability of HRG-β1 to stimulate erbB2 and erbB3 tyrosine phosphorylation was used as one of its biological functions when it was first isolated. Detection of $p180^{erbB3}$ and/or $p185^{erbB2}$ protein tyrosine phosphorylation by anti-phosphotyrosine antibodies using western blot analyses showed that the full extracellular domain HRG stable transfectants expressed secreted HRG proteins that phosphorylated p180/p185 proteins as did the positive control (commercially available recombinant HRG-β1) (Fig. 9). This was not detected in the parental or vector control cell lines. These data indicate that we have established stable transfectants of full extracellular domain of HRG in MDA-MB-435 and MCF-7 cells. Moreover, the transfectants secreted HRG that is functional.

Tasks 5 –7 were proposed for second supporting year.

Objective 3. To identify the minimum domains in HRG-β1 that is sufficient for inhibition of invasion/metastasis

Task 8: Months 7-10 (student 2): Use PCR-based mutagenesis technique to generate a series of HRG-β1 extracellular domain mutants.
Task 9: Months 11-12 (student 2): Subcloned HRG-β1 extracellular domain mutants into pcDNA3 expression vector.

As mentioned above, it took student 2 (with some help from student 1) more than one year to get the paper on HRG-β1 regulation of breast cancer aggregation published in *Cancer Research (* 59: 1620-1625, April, 1999, see Appendix B). Student 2 only had time to work on part of the Tasks 8 and 9. Basically, we used PCR-based technique to generate the egf-like domain of HRG-β1. We then subcloned the egf-like domain of HRG-β1 into the pSecTag2 secretion vector that contained histidine and myc tags (Fig 10). We did not use pcDNA3 expression vector because it does not allow the egf-like domain of HRG-β1 to be secreted. We plan to use similar strategy to clone other mutants of HRG-β1 in the second funding period. Currently, we are transfecting the egf-like domain expression vector into MDA-MB-435 and MCF-7 cells.

Key Research Accomplishments

We have fulfilled most of the proposed tasks for the first year of the grant support.
1. We demonstrated that the recombinant HRG-β1 can transcriptionally upregulate gelatinases activity.

2.We found that HRG-β1 induces the aggregation (a metastasis associated property) of breast cancer cells via activation of PI-3-K but independent of ERK (*Cancer Res.* 59: 1620-1625, 1999).
3.We subcloned the extracellular domain of the full length HRG-β1 into the pSecTag2 expression vector, transfected it into MDA-MB-435 and MCF-7 cell, and established stable transfectants.
4. We have cloned the egf-like domain of HRG-β1 to pSecTag expression vector and are transfecting it into MDA-MB-435 and MCF-7 cells.

Reportable Outcomes:

-manuscripts, abstracts, presentations
We have published two papers under the grant support. See Appendix B.

-patents and licenses applied for and/or issued None

-degrees obtained that are supported by this award None

-development of cell lines, tissue or serum repositories

We have established several stable transfectants expressing the full extracellular domain of HRG.

-informatics such as databases and animal models None

-funding applied for based on work supported by this None

-employment or research opportunities applied for and/or received on experiences/training supported by this award None

Conclusions:

The research supported by the first year of funding has been very productive. We have fulfilled most of the proposed tasks for the first year of the grant support. We demonstrated that the recombinant HRG-β1 can transcriptionally upregulate gelatinases activity in MCF-7 and SKBR-3 breast cancer cells but not in MDA-MB-435 or MDA-MB-231 cells. We found that HRG-β1 also inhibit invasion of MDA-MB-231 cells but not MCF-7 and SKBR-3 breast cancer cells. We found that HRG-β1 induces the aggregation (a metastasis associated property) of breast cancer cells via activation of PI-3-K but independent of ERK (*Cancer Res.* 59: 1620-1625, 1999). To determine the effect of HRG-β1 in metastasis *in vivo*, we subcloned the extracellular domain of the full length HRG-β1 into the pSecTag2 expression vector, transfected it into MDA-MB-435 and MCF-7 cell, and established stable transfectants. To further delineate the domain(s) of HRG-β1 that regulates invasion/metastasis of breast cancer cells, we have also cloned the egf-like domain of HRG-β1 to pSecTag2 expression vector. We are currently transfecting the egf-like domain of HRG-β1 expression vector into MDA-

MB-435 and MCF-7 cells to establish stable transfectants. These initial works have paved a productive avenue for the next grant-support year, when we will gain more insights regarding the role of HRG-β1 in breast cancer metastasis.

Note: Our first year *in vitro* data strongly suggest that the role of HRG-β1 on metastasis may be cell line specific and significantly depend on the erbB3 receptor levels of breast cancer cells. We observed that HRG-β1 can have different effects on MDA-MB-435 and MDA-MB-231 erbB3 low cells versus MCF-7 and SKBR-3 erbB3 high cells. Therefore, we feel strongly that we need to do *in vivo* experiments on both erbB3 low (MDA-MB-435) and high (MCF-7) expressing breast cancer cells. Our additional efforts to also establish HRG-β1 stable transfectants in MCF-7 cells (please see our report on task 4) will double the amount of work compared to that of originally proposed. This may reduce our time to work on the Objective 3. We will adjust our priority with the key question of the Idea proposal in mind, i.e., to determine whether HRG-β1 can inhibit breast cancer cell metastasis and in what cell contest it may do so. We may need to reduce our efforts on some less critical experiments.

Reference:

Tan, M., Grijalva, R. and **Yu, D.** Activation of phosphatidylinositol 3-Kinase by Heregulin β1 induces the aggregation of MCF-7 breast cancer cells independent of extracellular signal-regulated kinase. *Cancer Res.* 59: 1620-1625, 1999.

Appendices

A. Ten figures cited in this report.

B. Reprints

1. Reprint of a paper partially supported by the Idea Award published in *Cancer Res.* 59: 1620-1625, 1999.

2. Reprint of a paper partially supported by the Idea Award published in *Molecular Cell*, 2: 581-591, 1998.

Appendix A

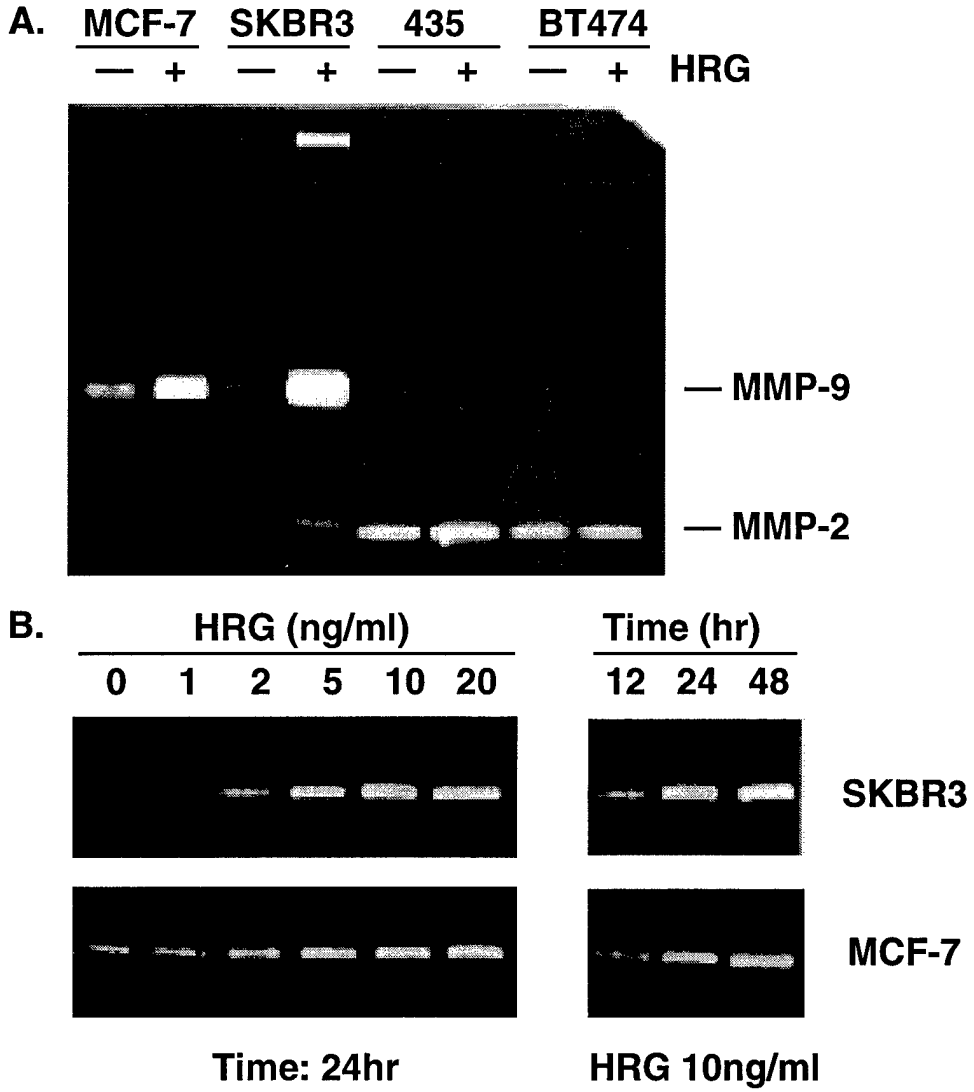

Fig.1 Heregulin-β1 (HRG) does not activate MMP-9 in MDA–MB-435 and BT474 breast cancer cells but activates MMP-9 in MCF-7 and SKBR3 cells. (A) Zymographic assay of MMP-9 activation in response to HRG stimulation. Breast cancer cells were cultured to 80% confluence and changed to serum-free medium for 12 hr. Cells were then stimulated with or without HRG beta1 for 24 hr. Conditioned media were collected and concentrated by Centricon-30, separated by SDS-PAGE under non-reducing condition. The gel was washed away of SDS and incubated in a reaction buffer containing calcium and zinc at 37°C for 24 hr. The gelwas stained with Coommassie Blue and destained. (B) Time and dose dependent activation of MMP-9 by HRG in SKBR3 and MCF-7 cells. Zymography was performed in a similar way as described in (A) except different HRG concentrations and incubation time were used.

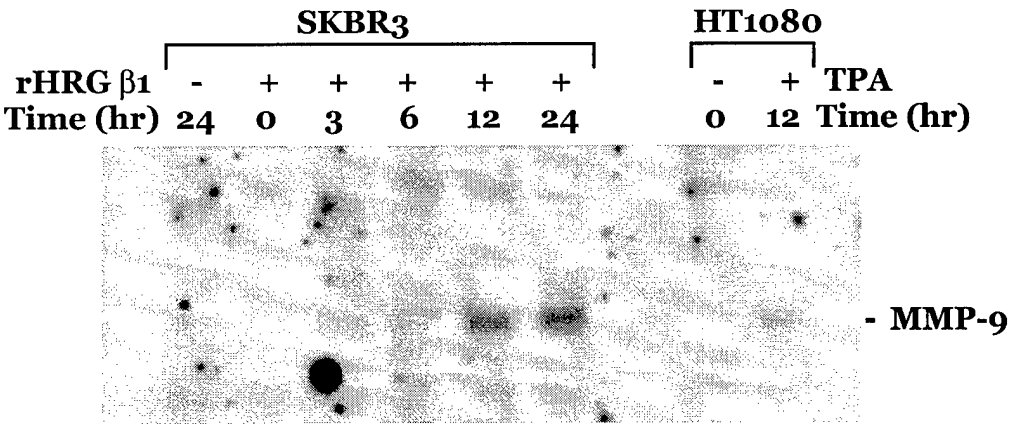

Fig.2 Northern blot analysis of MMP-9 after HRG stimulation. SKBR3 cells were cultured to 80% confluence and starved for 12 hr before stimulated with HRG. At different time points, the cells were harvested and total RNA prepared. 20μg of total mRNA were separated on the agarose gel and transferred to nylon membrane. A [^{32}P] labeled DNA probe specific for MMP-9 but not other MMPs was used to hybridize the membrane. After wash, the membrane was exposed to X-ray film. 10μg of total RNA from HT1080 cells treated with TPA were used as a positive control.

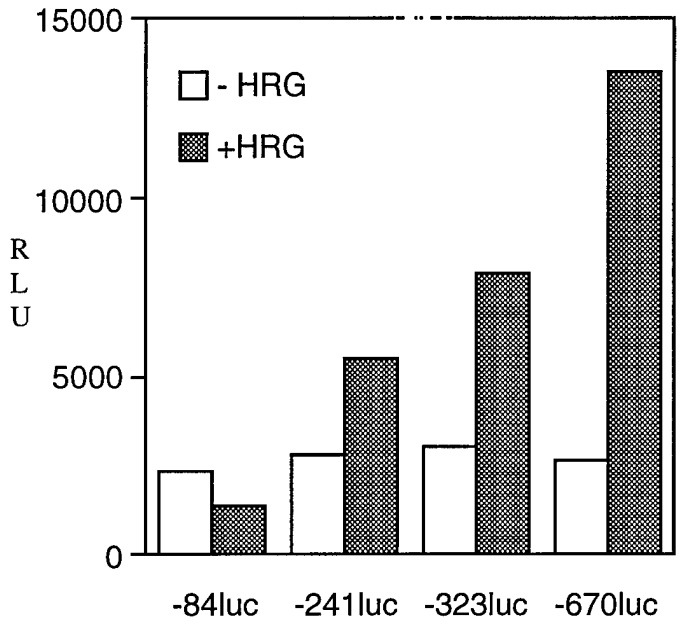

Fig.3 Searching for HRG-responsive cis-elements on MMP-9 promoter by reporter luciferase assay. MCF-7 cells were grown in 6cm culture dish to 80% confluce in DMEM/F12 medium containing 10% FBS. 2μg pCMV-lacZ and 6.5μg pMMP-luc(-84, -241, -323, -670) were cotrasfected by calcium phosphate method. 5 hours post-transfection, cells were washed and starved in serum-free media for 12 hours. The cells were then treated with or without recombinant HRG beta1 (10 ng/ml) for 24 hours. The cells were harvested in 250μl reporter lysis buffer (Promega). After one round freeez-thaw the cell pellet were spun down and supernatant used for luciferase assay.

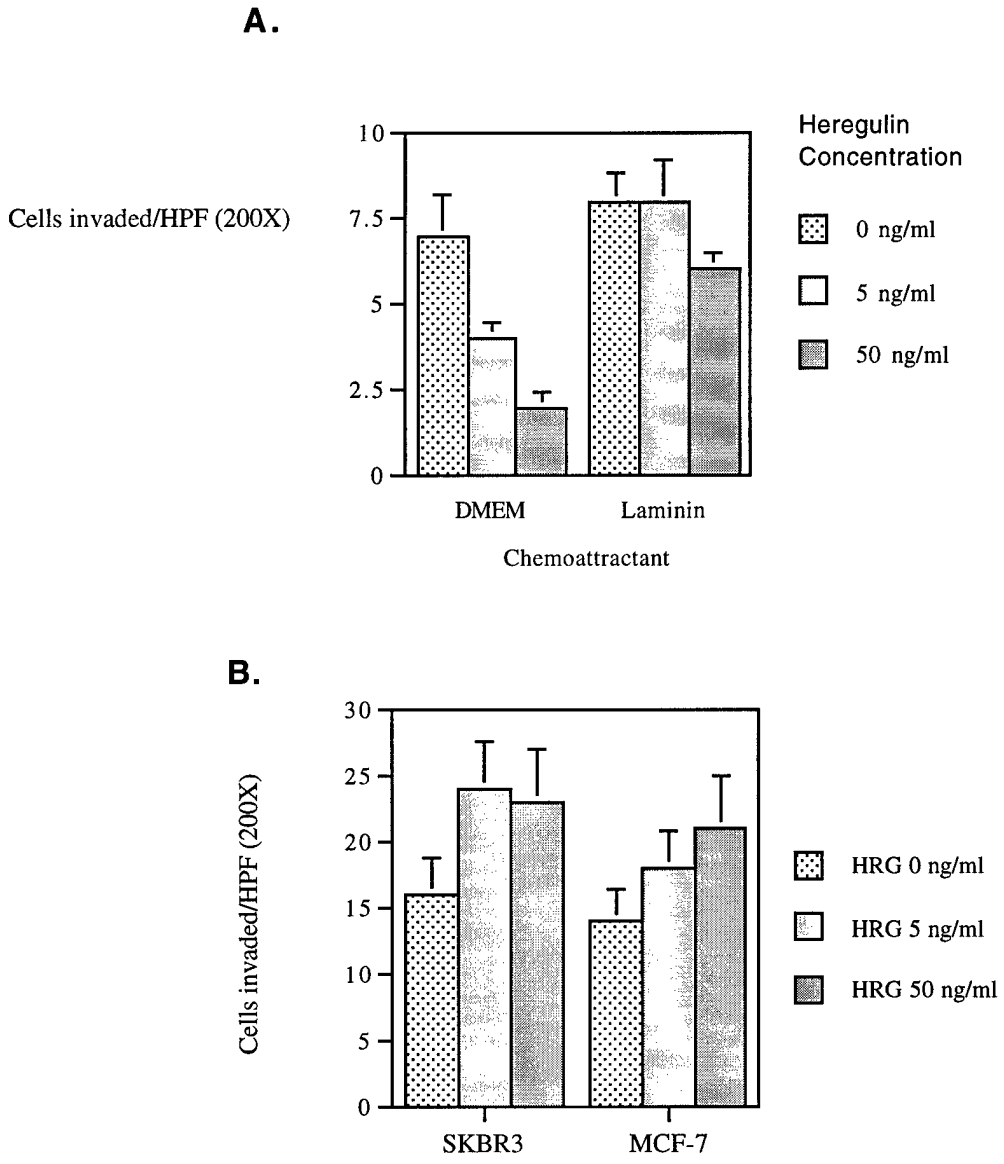

Fig. 4 (A) Decreased Invasion of MDA-MB-231 and (B) increased invasion of SKBR3, MCF-7 cells through Matrigel by Heregulin-β1. Invasion was measured using 24-well BioCoat Matrigel Invasion Chambers (Becton Dickinson Labware, MA) with an 8 μm-pore polycarbonate filter coated with Matrigel. The lower chamber contained 0.6 ml laminin (40 μg/ml) as chemoattractant. The cells (1 X 105 cells in 0.1 ml Dulbecco's Modified Eagle's Medium/Ham's F-12 with 0, 5, or 50 ng/ml recombinant human heregulin-β1) were placed in the upper chamber and incubated for 72 h at 37°C. After incubation, the cells were fixed with 3% glutaraldehyde and stained with Giemsa. The Matrigel-invading cells were counted in three high-power fields.

A. anti-HER3

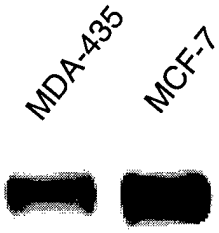

B. anti-Heregulin

Fig. 5. Immunoblot analysis of HER3 (erbB3) protein level in cell lysates and HRG-β1 in conditioned medium, from MDA-MB-435 and MCF-7 cells. 100 μg of protein lysate or 400 μg of conditioned medium from each sample was electrophoresed on 8% SDS-PAGE and transferred to nitrocellulose filters and probed with the monoclonal antibodies against (A) HER3 and (B) heregulin (NeoMarkers, Fremont). T47D cell lysate was used as positive control for HRG.

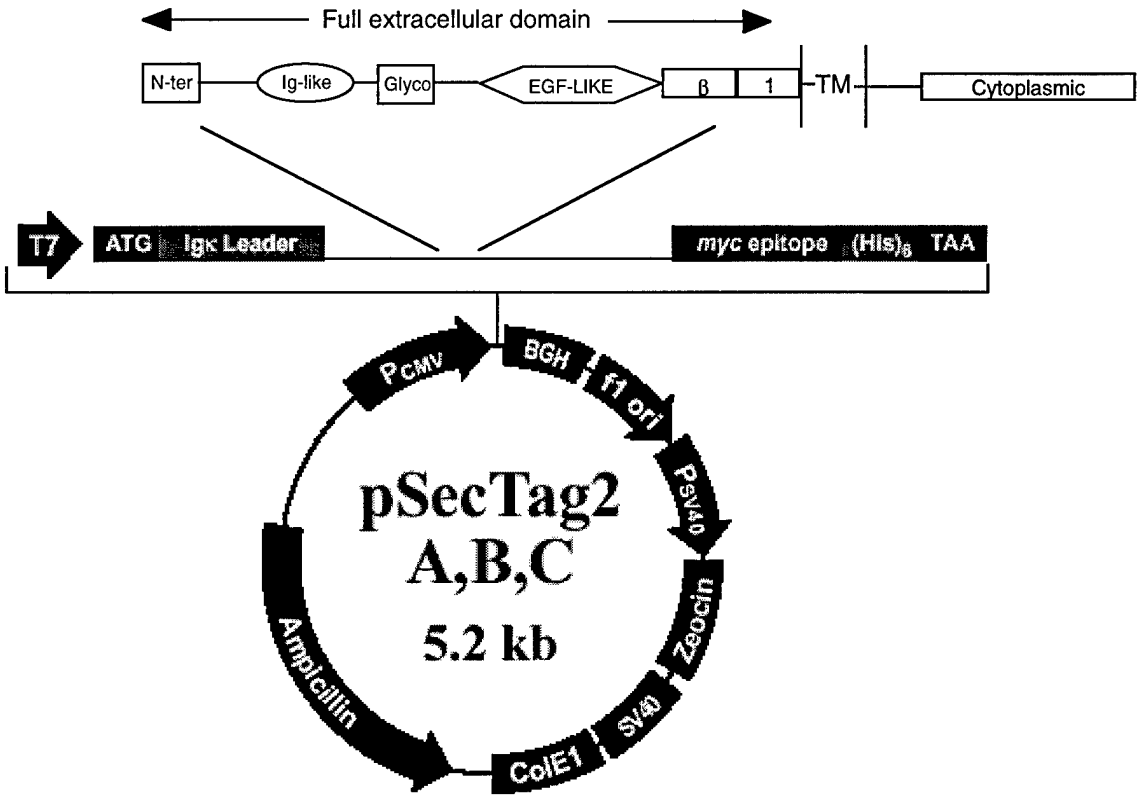

Fig. 6. The full extracellular domain of heregulin-β1 (HRG-β1) was subcloned into the expression vector pSecTag2 (Invitrogen, Carlsbad).

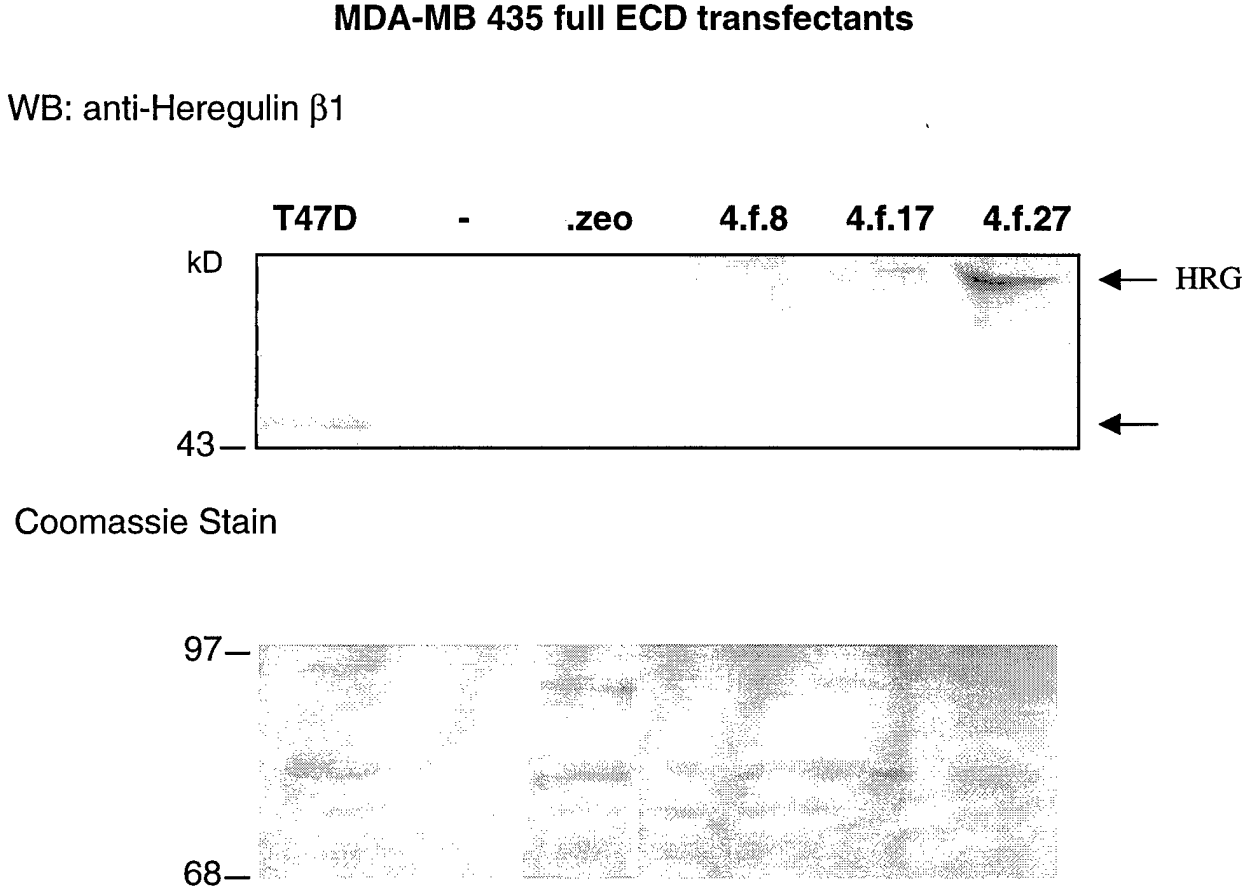

Fig. 7 Immunoblot analysis of the full extracellular domain heregulin-β1 secreted proteins in conditioned medium from MDA-MB-435 stable transfectants (4.f.8, 4.f.17, 4.f.27) and vector alone (zeo) cells. Conditioned medium from serum-starved cells was concentrated and 400 μg from each sample was electrophoresed by SDS-PAGE. The lower portion of the gel was transferred to nitrocellulose, and probed with anti-heregulin antibody (NeoMarkers, Fremont). The upper portion of the gel was stained with coomassie blue for loading control purposes. Note: the exogenous HRG proteins expressed in transfectants are larger in size than endogenous HRG in T47D cells. This is due to the additional leader sequences and various tags added to it.

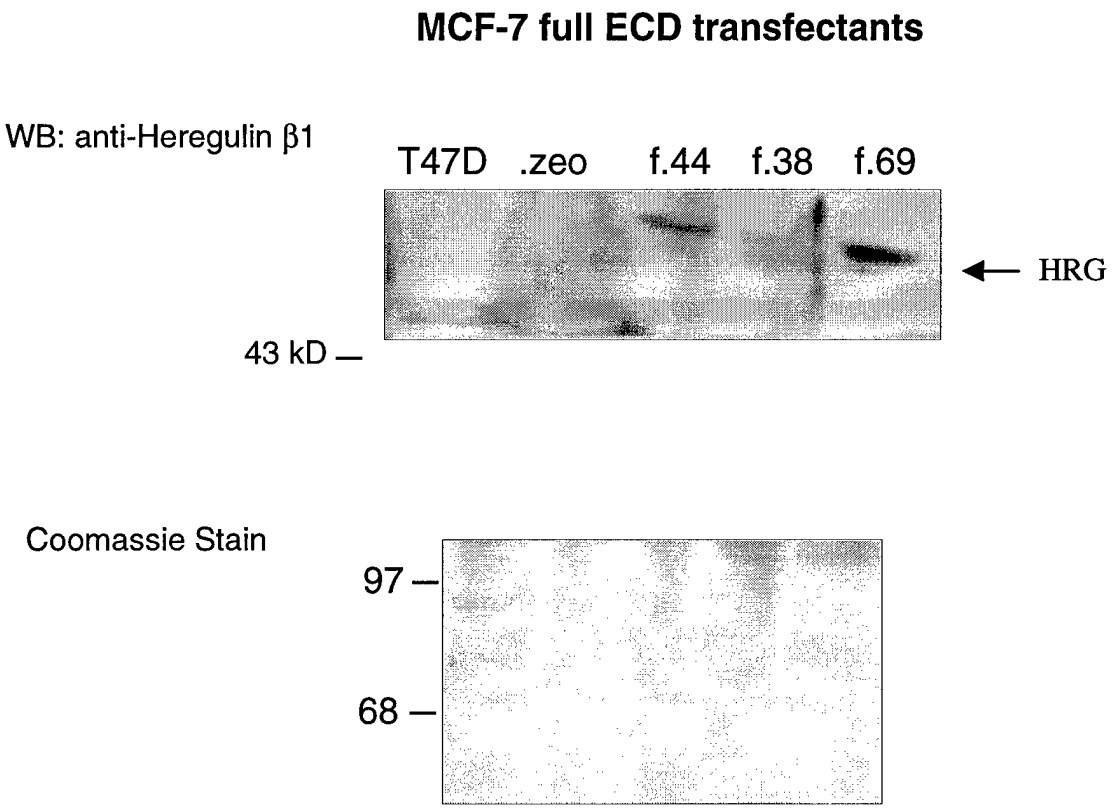

Fig. 8 Immunoblot analysis of the full extracellular domain heregulin-β1 secreted proteins in conditioned medium from MCF-7 stable transfectants (f44, f38, f69) and vector alone (zeo) cells. Conditioned medium from serum-starved cells was concentrated and 400 μg from each sample was electrophoresed by SDS-PAGE. The lower portion of the gel was transferred to nitrocellulose, and probed with anti-heregulin antibody (NeoMarkers, Fremont). The upper portion of the gel was stained with coomassie blue for loading control purposes.

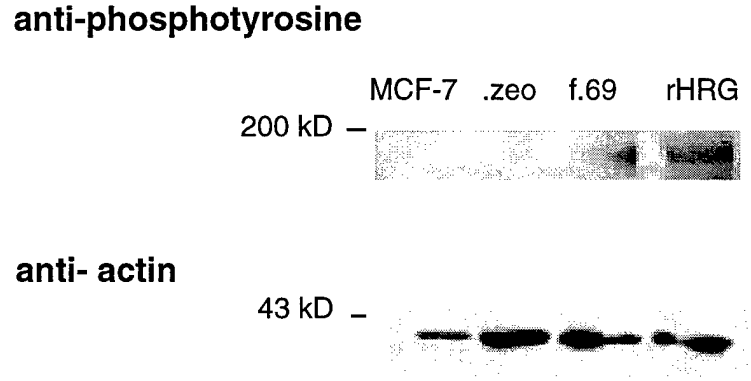

Fig. 9. Immunoblot analysis of tyrosine phosphorylation by heregulin-β1 full extracellular domain protein. Conditioned medium from serum-starved stable transfectants, parental, and vector control cells was concentrated and 400 μg from each sample was used to treat MCF-7 parental cells. Protein lysates (150 μg) from treated cells were electrophoresed on an 8% SDS-PAGE gel which was transferred to nitrocellulose and probed with anti-phosphotyrosine PY20 antibody (Transduction Laboratories, Lexington). The lower portion of the nitrocellulose membrane was probed with anti-b-actin antibody for loading control.

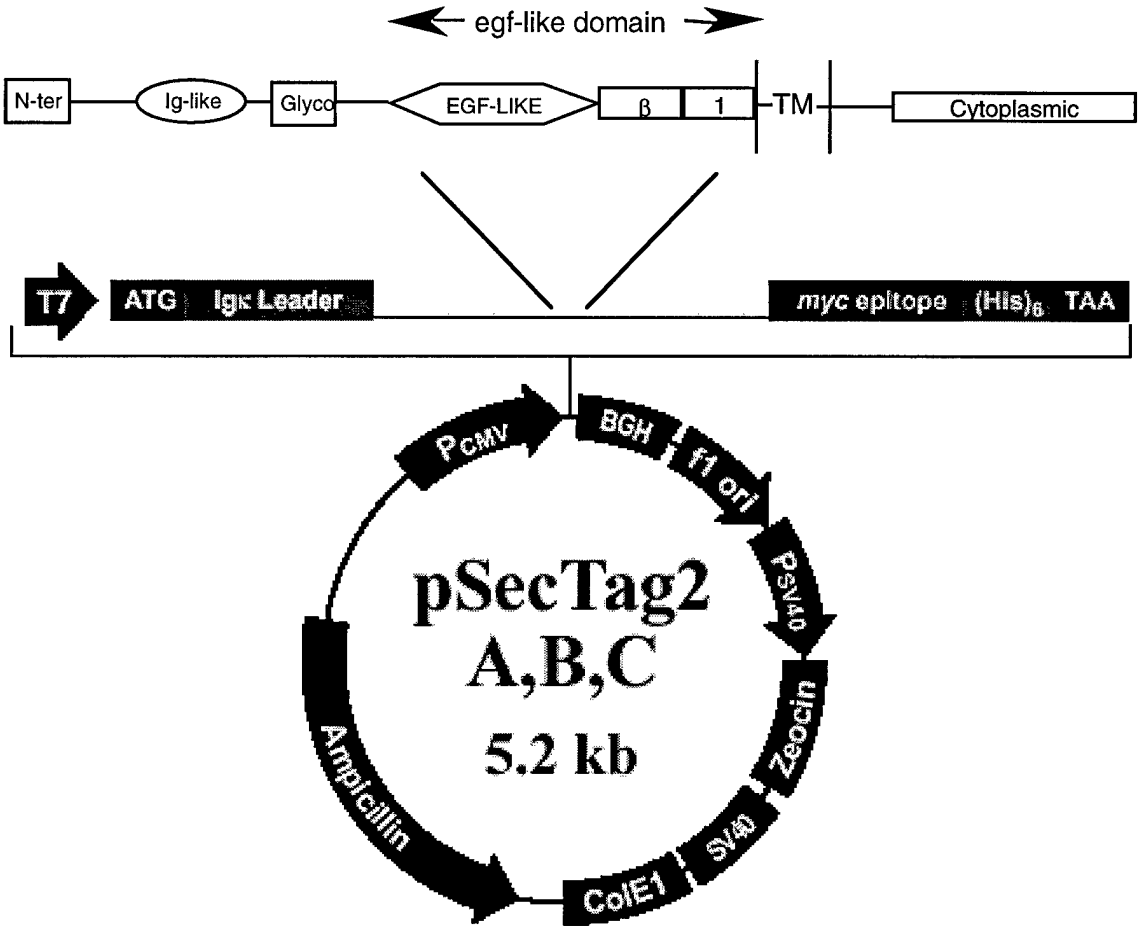

Fig. 10. The egf-like domain of heregulin-β1 (HRG-β1) was subcloned into the expression vector pSecTag2 (Invitrogen, Carlsbad).

[CANCER RESEARCH 59, 1620–1625, April 1, 1999]

Heregulin β1-activated Phosphatidylinositol 3-Kinase Enhances Aggregation of MCF-7 Breast Cancer Cells Independent of Extracellular Signal-regulated Kinase[1]

Ming Tan, Rebecca Grijalva, and Dihua Yu[2]

From the Department of Surgical Oncology and The Breast Cancer Basic Research Program, The University of Texas M. D. Anderson Cancer Center, Houston, Texas 77030

ABSTRACT

Heregulin (HRG) is a family of polypeptide growth factors derived from alternatively spliced genes. HRG can bind to receptor tyrosine kinases erbB3 and erbB4, thereby inducing erbB3 and erbB4 heterodimerization with erbB2, leading to receptor tyrosine phosphorylation and activating downstream signal transduction. Cell-cell homophilic adhesion (cell aggregation) is important in determining the structural organization and behavior of cells in tissues. In addition, tumor cell homophilic adhesion may affect invasive and metastatic potentials of cells. We report that HRG-β1 can enhance aggregation of MCF-7 and SKBR3 human breast cancer cells. While investigating the downstream signals involved in HRG-β1-enhanced cell aggregation, we observed that HRG-β1 induced tyrosine phosphorylation of erbB2 and erbB3 receptor heterodimers and increased the association of the dimerized receptors with the 85-kDa subunit of phosphatidylinositol 3-kinase (PI3K). HRG-β also increased the kinase activities of extracellular signal-regulated protein kinase (ERK) and PI3K in these cells. By using the mitogen-activated protein kinase/ERK 1 (MEK1) inhibitor PD98059 and PI3K inhibitors wortmannin and LY294002, we found that blocking the MEK1-ERK pathway had no effect on HRG-β1-enhanced cell aggregation; however, blocking the PI3K pathway greatly inhibited HRG-β1-mediated cell aggregation. Our study indicated that the HRG-β1-activated MEK1-ERK pathway has no demonstrable role in the induction of cell aggregation, whereas HRG-β1-activated PI3K is required for enhancing breast cancer cell aggregation. Because aggregation can contribute to invasion/metastasis phenotype of cancer cells, our results have provided one mechanism by which HRG-β1-activated signaling of erbB receptors may affect invasive/metastatic properties of MCF-7 and SKBR3 breast cancer cells.

INTRODUCTION

The erbB family of receptor tyrosine kinases has four known members: erbB1 (EGF[3] receptor), erbB2, erbB3, and erbB4 (1–4). The erbB receptors are widely expressed in epithelial, mesenchymal, and neuronal tissues and play fundamental roles during development. Their aberrant expression is frequently observed in human malignant diseases (5, 6). The precise mechanism by which erbB receptors are involved in human cancer progression remains poorly understood, but, presumably, it involves signal transduction pathways that are activated by ligand binding.

HRG, also called neu differentiation factor, is a family of polypeptide growth factors derived from alternatively spliced genes (7–10). HRG can bind to receptor tyrosine kinases erbB3 and erbB4, thereby inducing erbB3 and erbB4 heterodimerization with erbB2, receptor tyrosine phosphorylation, and downstream signal transduction (2, 11, 12). Several signal transduction pathways activated by HRG have been reported recently. Activation of PI3K, ERK, and the stress-activated protein kinase/c-Jun N-terminal kinase have been observed in various systems (13–16). Studies of breast cancer cell lines have revealed that the physiological effects of HRG are diverse and cell type-dependent (9, 17). In addition to regulating cell growth and differentiation, HRG may be involved in regulation of other biological behaviors of cancer cells, such as apoptosis (18), cell adhesion, migration, and invasion (19, 20); but, the overall picture of its biological effects is still not clear. Moreover, little is known regarding the integration of HRG-activated signals leading to various biological effects.

Cell adhesion is crucial for maintaining the structural integrity of tissues. Cell-matrix adhesion is mediated by heterophilic interactions between cell-surface receptors and their matrix ligands, whereas cell-cell adhesion (cell aggregation) primarily involves direct homophilic interactions between cell-surface molecules such as the cadherins (21). Cell-adhesion molecules do not merely offer structural anchors for cells, but also transmit signals that are integrated with other cellular activities in the coordination of major aspects of cell behavior, including proliferation, differentiation, apoptosis, and cell movement (21, 22).

We report here that HRG-β1 can enhance aggregation of MCF-7 and SKBR3 human breast cancer cells. We demonstrated that PI3K is required for the induction of cell aggregation in response to HRG-β, but that the mitogen-activated protein kinase (ERK) activated by HRG-β has no demonstrable role in the induction of cell aggregation.

MATERIALS AND METHODS

Materials. Recombinant human HRG-β was purchased from NeoMarkers (Fremont, CA). Wortmannin, LY294002, and PD98059 were purchased from Calbiochem (La Jolla, CA). Antibodies against erbB2 were from Oncogene Science Products (Cambridge, MA); antibodies against erbB3 were from NeoMarkers; antibodies against PI3K 85-kDa subunit were from Upstate Biotechnology Inc. (Lake Saranac, NY); antibodies against phosphotyrosine and ERK2 were from Santa Cruz Biotechnology (Santa Cruz, CA); and antibodies against phospho-ERK were from New England Biolabs (Beverly, MA).

Cell Culture. The human breast carcinoma cell lines MCF-7 and SKBR3 were purchased from the American Type Culture Collection (Manassas, VA) and maintained in DMEM/F12 (Life Technologies, Inc., Grand Island, NY) supplemented with 10% fetal bovine serum (Life Technologies, Inc.).

Cell Aggregation Assay. Cells in subconfluent cultures were serum-starved for 24 h, treated with chemical kinase inhibitors or their solvent (DMSO), then detached from tissue culture dishes and washed with serum-free medium. Each well of a 24-well low-binding affinity tissue culture plate (Costar Corp., Cambridge, MA) contained 500 μl of single-cell suspension at the concentration of 5×10^4 cells/ml in DMEM/F12 containing 0.5% BSA. Cells were plated in the presence (5 or 50 ng/ml) or absence of HRG-β or EGF. Plates were incubated at 4°C or 37°C on a rotating platform for 30 min. Aggregated cell mixtures were fixed with 2% glutaraldehyde. The aggregates were defined as cell clumps containing more than five cells. Aggregates in four randomly selected high-power fields were counted using light microscopy.

Received 9/14/98; accepted 1/28/99.

The costs of publication of this article were defrayed in part by the payment of page charges. This article must therefore be hereby marked *advertisement* in accordance with 18 U.S.C. Section 1734 solely to indicate this fact.

[1] Supported by National Cancer Institute Grant CA60488 (to D. Y.), Grant DAMD17-98-18338 from the United States Department of Defense Breast Cancer Research Program (to D. Y.), and by the M. D. Anderson Breast Cancer Research Program Fund (to D. Y.). M. T. is a recipient of a predoctoral fellowship from the United States Department of Defense Breast Cancer Research Program (DMDA17-97-1-7259).

[2] To whom requests for reprints should be addressed, at Department of Surgical Oncology, Box 107, The University of Texas M. D. Anderson Cancer Center, 1515 Holcombe Boulevard, Houston, TX 77030. Phone: (713) 792-3636; Fax: (713) 794-4830.

[3] The abbreviations used are: EGF, epidermal growth factor; HRG, heregulin; PI3K, phosphatidylinositol 3-kinase; ERK, extracellular signal-regulated kinase; MEK, mitogen-activated kinase/ERK.

Preparation of Cell Lysates and Immunoprecipitates. Cells at 70–80% confluency were starved in serum-free medium for 24 h and treated with or without chemical kinase inhibitors, then stimulated without or with HRG-β (5 or 50 ng/ml) at 37°C for 5 min. The cells were washed and lysed in lysis buffer (23), and the insoluble materials were removed by centrifugation. Equal amounts of protein were incubated with the indicated antibodies for 1 h at 4°C and precipitated with protein A-Agarose. The immunoprecipitates were washed four times with the lysis buffer and eluted by boiling for 5 min in sample buffer before separation by SDS-PAGE.

Western Blot Analysis. Proteins were separated by SDS-PAGE and transferred to a nitrocellulose membrane (Bio-Rad Laboratories, Hercules, CA). Western blotting was performed using the enhanced chemiluminescence detection system (Amersham Corp., Arlington Heights, IL). Horseradish peroxidase-conjugated antibodies against mouse IgG or rabbit IgG (Jackson ImmunoResearch Laboratories, West Grove, PA) were used as secondary antibodies.

PI3K Assay. Cells at 70–80% confluency were stimulated with or without HRG-β, lysed, and immunoprecipitated with anti-erbB3 antibody, as described above. The PI3K assay was performed essentially as previously described (23), with minor modification.

ERK Assay. HRG-treated or -untreated cells (70–80% confluent) were lysed and immunoprecipitated with anti-ERK2 antibody, as described above. The ERK assay was performed as described previously (24).

RESULTS

Enhancement of Human Breast Cancer Cell Aggregation by HRG-β. HRG-β was previously shown to enhance invasiveness of SKBR3 breast cancer cells (25), and cell aggregation was suggested to play an important role in cancer cell invasion/metastasis (26–28). Here, we asked whether HRG-β may enhance breast cancer cell aggregation. To this end, 5 or 50 ng/ml of HRG-β was added to the cell suspension of serum-starved MCF-7 human breast cancer cells. We found that HRG-treated MCF-7 cells formed dramatically more

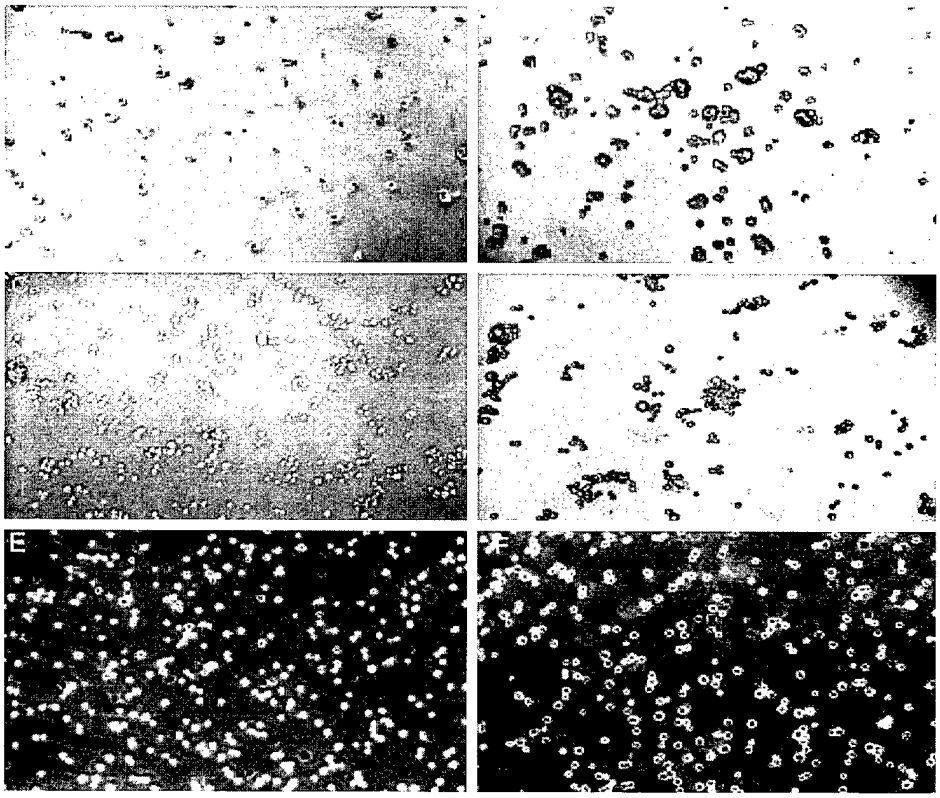

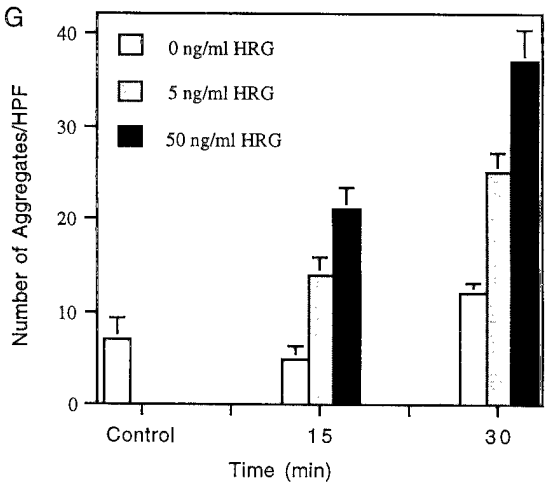

Fig. 1. Homophilic aggregation of MCF-7 and SKBR3 breast cancer cells was enhanced by HRG-β1, but not by EGF. Single-cell suspension (500 μl: 5 × 10^4 cells/ml in DMEM/F12 medium containing 0.5% BSA) in the presence or absence of HRG-β or EGF were plated into each well of a 24-well low-binding plate. The plate was incubated at 4°C or 37°C on a rotating platform for 30 min. Photographs were taken using a Nikon N6006 camera (magnification, ×200). *A* and *B*, MCF-7 cells were treated with 0 or 5 ng/ml HRG-β. *C* and *D*, SKBR3 cells were treated with 0 or 5 ng/ml HRG-β. *E* and *F*, MCF-7 cells were treated with 0 or 5 ng/ml EGF. *G*, MCF-7 cells were serum-starved and detached from tissue culture dishes using 10 mM EDTA and 0.1% BSA in PBS. Single-cell suspensions (500 μl: 5 × 10^4 cells/ml in DMEM/F12 medium containing 0.5% BSA) in the absence or presence of 5 ng/ml or 50 ng/ml HRG-β were plated into wells of a 24-well low-binding affinity plate. The plate was incubated at 37°C on a rotating platform for 30 min. Cells were then fixed and quantitated. Untreated control cells were fixed immediately after plating. The number of cell aggregates represents the average number determined from four random high-power fields.

aggregates than those of untreated cells (Fig. 1, *A* and *B*). The same effect was seen in the human breast cancer cell lines SKBR3 (Fig. 1, *C* and *D*), MDA-MB-435, and MDA-MB-231 (data not shown). To test whether the HRG-β-enhanced aggregation is an energy-dependent process, we performed the aggregation assay at both 4°C and 37°C. MCF-7 cells formed aggregates at both temperatures (data not shown), indicating that the aggregation process is not energy-dependent. The quantitative measures of aggregation assays are shown in Fig. 1*G*, which demonstrated that the enhancement of cell aggregation by HRG-β is concentration-dependent. This process is HRG-β-specific, because EGF does not enhance MCF-7 and SKBR3 cell aggregation under the same conditions (Fig. 1, *E* and *F*). These results indicated that HRG-β can enhance human breast cancer cell aggregation *in vitro* and that the effect is HRG-β–specific.

HRG-β Enhances Tyrosine-phosphorylation of erbB2 and erbB3 Heterodimers and Their Association with the 85-kDa Subunit of PI3K. To investigate the downstream signals involved in HRG-β-enhanced aggregation, we examined HRG-β-mediated activation of erbB2 and erbB3 in the MCF-7 and SKBR3 cell lines. The erbB2 and erbB3 receptors from HRG-β-treated or -untreated MCF-7 and SKBR3 cells were immunoprecipitated with anti-erbB2 and anti-erbB3 antibodies; then, Western-blot analysis with antiphosphotyrosine antibody was performed to measure tyrosine phosphorylation of erbB2 and erbB3 heterodimers (Fig. 2, *A* and *B*). Treatment of MCF-7 and SKBR3 cells with HRG-β dramatically increased tyrosine phosphorylation levels of anti-erbB3 immunoprecipitates (Fig. 2*B*) and moderately increased those of anti-erbB2 immunoprecipitates (Fig. 2*A*). To determine the association of the 85-kDa subunit of PI3K (p85) with erbB2 and erbB3 in these cells, we performed Western blot analysis of the anti-erbB2 and anti-erbB3 immunoprecipitates with anti-p85 antibody (Fig. 2, *A* and *B*). HRG-β stimulation greatly increased the p85 association with anti-erbB3 immunoprecipitates in both cell lines (Fig. 2*B*), and a moderate increase of the p85 association was seen in anti-erbB2 immunoprecipitates (Fig. 2*A*). These results indicate that HRG-β can activate erbB3 and erbB2 and, consequently, increase the association of p85 with erbB2 and erbB3 receptor dimers.

Activation of ERK and PI3K by HRG-β. Both ERK and PI3K have been reported to be involved in cell adhesion of several cell types (22, 29). Therefore, we examined whether HRG-β can activate ERK and PI3K in MCF-7 cells. MCF-7 cells were starved and treated with HRG-β before kinase assays were performed. We found that ERK activity can be dramatically activated by different concentrations of HRG-β (Fig. 3*A*). We also tested the kinetics of ERK activation by Western blot analysis using phospho-ERK-specific antibodies. The results revealed that ERK activity increased within 5 min and was sustained at least for 30 min (Fig. 3*B*). Next, we examined whether HRG-β can activate PI3K in these cells. As shown in Fig. 3*C*, PI3K activity was greatly increased by HRG-β stimulation. Kinetic studies of PI3K activation revealed that PI3K activity began to increase 5 min after the addition of HRG-β and reached its highest level at 10 min, which was sustained for at least 30 min (Fig. 3*D*). These results indicate that HRG-β can activate both ERK and PI3K in MCF-7 cells and that both ERK and PI3K activation precede the induction of aggregation.

ERK Activation Is Not Required for HRG-β-stimulated Cell Aggregation. Using PD98059, a specific inhibitor of MEK1 (30, 31), we investigated whether interfering with the MEK1-ERK signaling pathway would inhibit HRG-β-enhanced cell aggregation. As demonstrated by both ERK assay (Fig. 4*A*) and Western analysis using phospho-ERK-specific antibodies (Fig. 4*B*), activation of ERK by HRG-β was inhibited in a concentration-dependent manner when the cells were treated with different concentrations of PD98059. We next

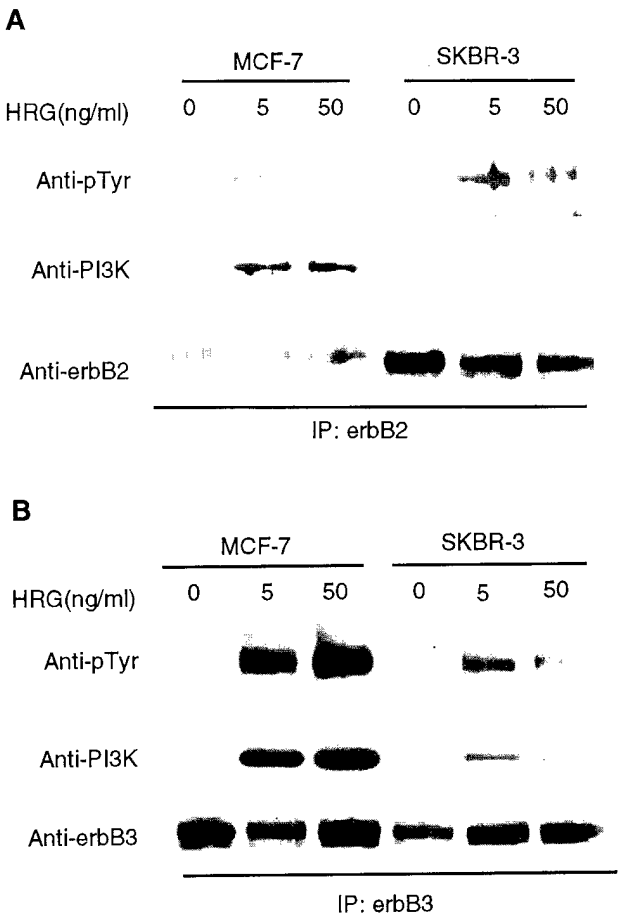

Fig. 2. HRG-β increases erbB2 and erbB3 heterodimer tyrosine-phosphorylation and their association with PI3K. Serum-starved MCF-7 and SKBR3 cells were treated with 0, 5, and 50 ng/ml HRG-β1 for 5 min. Cell lysates containing equal amounts of proteins were immunoprecipitated with antibodies against erbB2 (*A*) and erbB3 (*B*). Immunoprecipitates were separated on 8% SDS-PAGE and transferred to nitrocellulose membranes. The membranes were hybridized with antibodies against phosphotyrosine (*top*), stripped, and rehybridized with antibodies against the p85 PI3K subunit (*middle*), then stripped again, and rehybridized with antibodies against erbB2 (*A*, *bottom*) and erbB3 (*B*, *bottom*).

assessed the role of ERK in stimulating cell aggregation by HRG-β. As expected, 5 ng/ml HRG-β effectively enhanced aggregation of MCF-7 cells (Fig. 5, *A* and *B*), and PD98059 alone had no effect on MCF-7 cell aggregation (data not shown). It is notable that PD98059 had no inhibitory effect on HRG-β-enhanced MCF-7 cell aggregation (Fig. 5, *C* and *D*), indicating that induction of cell aggregation by HRG-β does not require activation of MEK1-ERK.

PI3K Activation Is Required for MCF-7 Cell Aggregation Enhanced by HRG-β. To examine the involvement of PI3K in HRG-β-enhanced MCF-7 cell aggregation, we tested whether a specific chemical inhibitor of PI3K, wortmannin (32, 33), would block HRG-β-enhanced MCF-7 cell aggregation by inhibiting PI3K activity. We treated the MCF-7 cells with varying concentrations of wortmannin. As shown in Fig. 4*C*, PI3K activity was inhibited by wortmannin in a concentration-dependent manner. Moreover, activation of PI3K by HRG-β at 4°C can also be inhibited by wortmannin (Fig. 4*D*). To determine the role of PI3K in enhancing cell aggregation by HRG-β, we examined the effect of wortmannin on HRG-β-mediated enhancement of MCF-7 cell aggregation. Wortmannin alone had no discernible effect on MCF-7 cell aggregation (data not shown), but it led to a concentration-dependent inhibition of HRG-β-enhanced MCF-7 cell aggregation (Fig. 5, *E* and *F*) compared with that without wortmannin (Fig. 5*B*). To confirm the PI3K requirement in HRG-β-enhanced

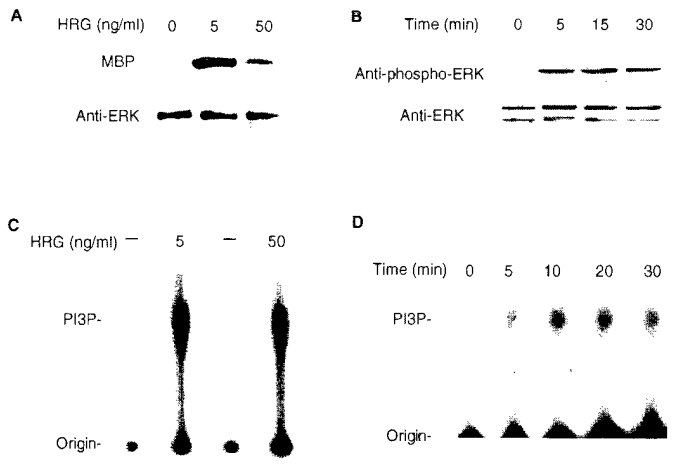

Fig. 3. Activation of ERK and PI3K by HRG-β. Serum-starved MCF-7 cells were treated with HRG-β at the indicated concentrations and time intervals. *A*, cell lysates were immunoprecipitated with anti-ERK2 antibodies, and the immunocomplexes were subjected to an ERK assay. Phosphorylation of myelin basic protein (*MBP*) by ERK was visualized by autoradiography (*top*). The ERK protein level was determined by Western blotting using anti-ERK antibody (*bottom*). *B*, cell lysates containing equal amounts of proteins were separated on 12% SDS-PAGE and transferred to nitrocellulose membranes. The membranes were hybridized with antibodies against phospho-ERK (*top*), stripped, and rehybridized with antibodies against ERK (*bottom*). *C* and *D*, cell lysates were immunoprecipitated with the anti-erbB3 antibodies and the immunocomplexes subjected to PI3K assay. The products of the reaction were analyzed by thin-layer chromatography and visualized by autoradiography. The product of PI3K, PI3P, is indicated on the *left*.

aggregation, we also tested the ability of LY294002 (34), a competitive PI3K inhibitor, to inhibit HRG-β-enhanced cell aggregation. Like wortmannin, LY294002 alone had no effect on MCF-7 cell aggregation (data not shown) but inhibited HRG-β-enhanced MCF-7 cell aggregation in a concentration-dependent manner (Fig. 5, *G* and *H*). These results indicate that PI3K is required for transducing HRG-β signals that result in MCF-7 cell aggregation.

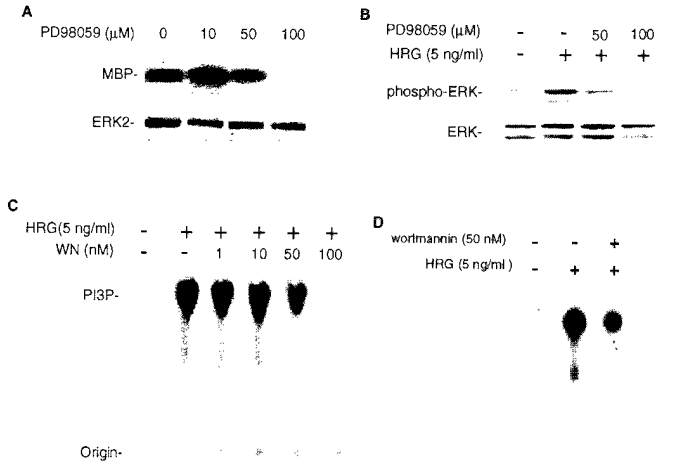

Fig. 4. Inhibition of ERK and PI3K by kinase inhibitors. *A*, serum-starved MCF-7 cells were pretreated with the indicated concentrations of PD98059 or its solvent DMSO for 2 h at 37°C before stimulation with 5 ng/ml HRG-β for 5 min. ERK2 was immunoprecipitated with anti-ERK2 antibodies and assayed *in vitro*. *MBP*, myelin basic protein. *B*, cell lysates containing equal amounts of proteins were separated on 12% SDS-PAGE and transferred to nitrocellulose membranes. The membranes were hybridized with antibodies against phospho-ERK (*top*), stripped, and rehybridized with antibodies against ERK (*bottom*). *C*, serum-starved MCF-7 cells were pretreated with the indicated concentrations of wortmannin (*WN*) or its solvent (DMSO) for 1 h at 37°C, then stimulated with 5 ng/ml HRG-β for 5 min at 37°C. PI3K was immunoprecipitated with anti-erbB3 antibodies and assayed *in vitro*. *D*, serum-starved MCF-7 cells were pretreated with indicated concentrations of wortmannin or its solvent (DMSO) for 1 h at 37°C, then stimulated with 5 ng/ml HRG-β for 5 min at 4°C. PI3K was immunoprecipitated with anti-erbB3 antibodies and assayed *in vitro*.

DISCUSSION

We report here that HRG-β1 can enhance aggregation of MCF-7 and SKBR3 human breast cancer cells. We have further investigated the molecular mechanisms underlying HRG-β-enhanced aggregation. Our results indicated that HRG-β induces phosphorylation of the erbB2 and erbB3 receptors and rapidly activates ERK and PI3K in MCF-7 cells. Although MEK1 inhibitor PD98059 effectively reduced HRG-β-mediated ERK enzyme activity, it failed to inhibit HRG-β-enhanced cell aggregation, indicating that HRG-β-activated ERK does not contribute to HRG-β-enhanced MCF-7 cell aggregation. However, blocking of PI3K by PI3K-specific chemical inhibitors wortmannin and LY294002 effectively inhibited HRG-β-enhanced MCF-7 aggregation, indicating that PI3K is required for HRG-β-enhanced cell aggregation.

Previous reports indicated that among the members of the erbB receptor family, erbB3 is a potent activator of PI3K (35–37). In MCF-7 and SKBR3 cells, erbB2 and erbB3 can be activated by HRG-β, and the resulting heterodimers of erbB2 and erbB3 can associate with the 85-kDa subunit of PI3K. However, the level of p85 associated with anti-erbB3 immunoprecipitates was dramatically higher than that of anti-erbB2 immunoprecipitates (Fig. 2, *A* and *B*), a result consistent with the previous studies. Compared with the SKBR3 cell line, MCF-7 cells expressed more erbB3, but less erbB2, and responded more strongly to HRG-β-enhanced aggregation (Fig. 1), indicating that erbB3 may play an important role in HRG-β-induced PI3K activation and cell aggregation.

Regulation of cell adhesion may occur at several levels, including affinity modulation, clustering, coordinated interactions with the actin cytoskeleton, and up-regulation of adhesion molecule expression (22). HRG has been reported to induce expression of integrin (38) and intercellular adhesion molecule 1 in human cancer cells (19). However, the time required for HRG-β-enhanced cell aggregation is shorter than the time needed for up-regulation of adhesion molecule expression. Therefore, functional activation of adhesion molecules and its consequences such as affinity modulation, clustering, and coordinated interactions with the actin cytoskeleton are more likely to be involved in the HRG-β-enhanced cell aggregation. By activating erbB receptors, HRG-β may send its signals through the PI3K pathway to activate these adhesion molecules, thereby inducing cell aggregation. Further investigation is needed to clarify which adhesion molecules are involved in this process. Another question that arises from these data are which downstream signaling molecules of PI3K are responsible for activating the adhesion molecules. Previous studies indicated that the small guanosine 5′ triphosphate-binding protein Rac is involved in cell adhesion and is downstream of PI3K (39–41). A recent study found that, in epithelial Madin-Darby canine kidney cells, Tiam1, an exchange factor for Rac, is localized to adherens junctions (42). These findings suggested an attractive notion that Rac may also play a role in the HRG-β-enhanced cell aggregation.

Cell-cell homophilic adhesion plays important roles in determining the structural organization and behavior of cells in tissues. Homophilic adhesion or aggregation is also important in tumor cell invasiveness and metastasis (26–28). Although reduced homotypic adhesion may contribute to dissemination of cells from the primary tumor, increased homotypic adhesion observed in circulating multicellular aggregates, also known as emboli, is required for lodgement, attachment, and growth of metastatic cells (43, 44). Positive correlations have been demonstrated between the propensity of tumor cells to undergo homotypic aggregation *in vitro* and their metastatic potential *in vivo* (45–47). Although only latter events of tumor cell metastasis (after tumor cell penetration into the blood

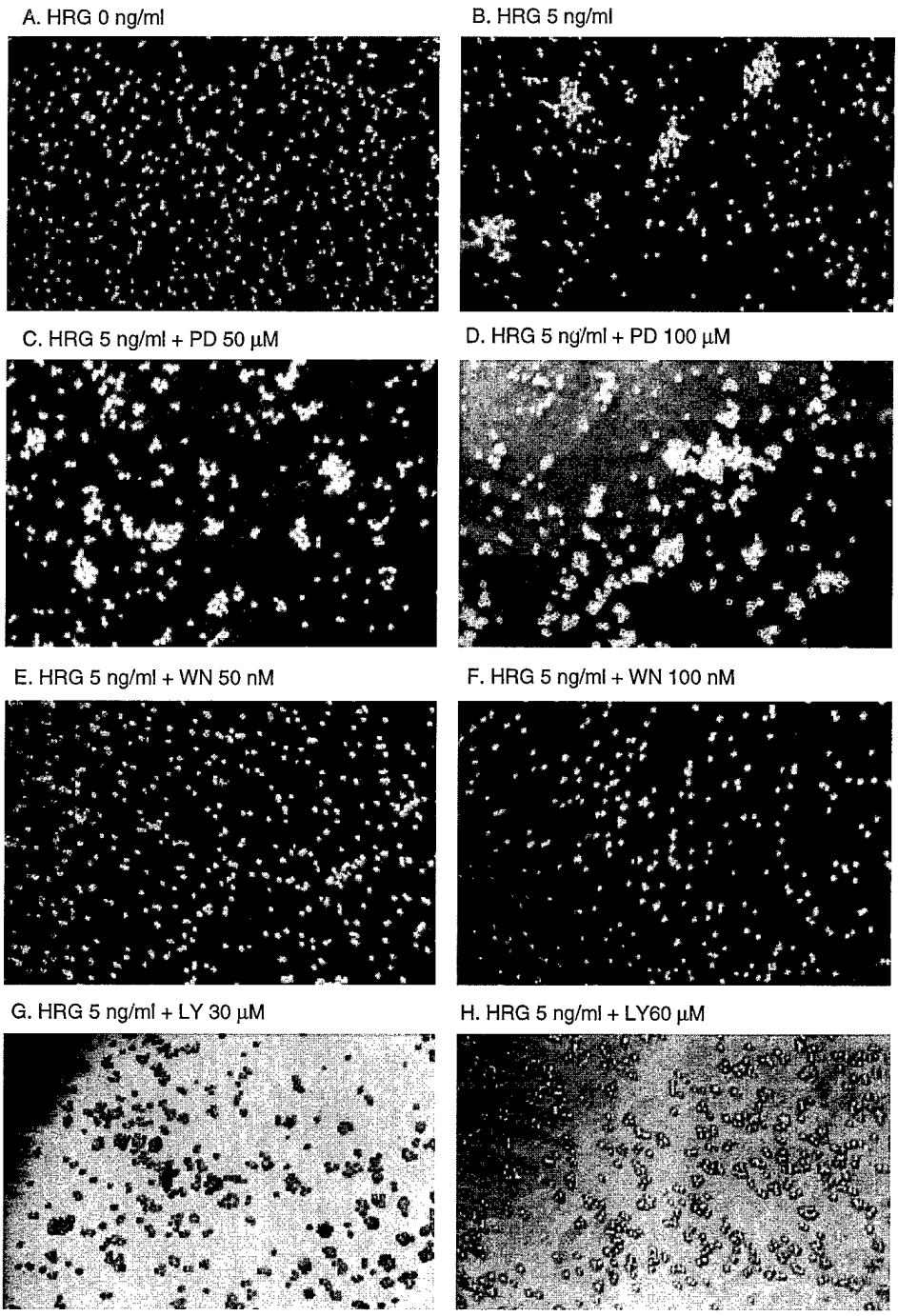

Fig. 5. HRG-β-enhanced MCF-7 cell aggregation was inhibited by wortmannin and LY294002, but not by PD98059. Cells were pretreated with indicated concentrations of PD98059 for 2 h or wortmannin or LY294002 for 1 h, detached from tissue culture dishes using 10 mM EDTA and 0.1% BSA in PBS, and washed with DMEM/F12 serum-free medium. Single-cell suspensions (500 μl; 5×10^4 cells/ml in DMEM/F12 medium containing 0.5% BSA) in the presence or absence of 5 ng/ml HRG-β were plated into wells of the 24-well low-binding affinity plate. The plate was incubated at 4°C on a rotating platform for 30 min. *PD*, PD98059; *WN*, wortmannin; *LY*, LY294002. Photographs were taken using a Nikon N6006 camera (magnification, ×200).

vessels) were tested in these previous studies, the work provided evidence that homophilic cell aggregation has an important role in tumor cell invasion and metastasis. The overall net effect of HRG-β on human breast cancer cell invasion/metastasis remains unclear, the ongoing studies in our laboratory will continue to focus on this issue.

Our finding that PI3K mediates MCF-7 cell aggregation enhanced by HRG-β identified PI3K as a new target in modulating human breast cancer cell aggregation. It may provide another clue to the control of human breast cancer cell invasion and metastasis.

ACKNOWLEDGMENTS

We thank Dr. Mien-Chie Hung for critical reading of the manuscript and Lore Feldman for editorial assistance.

REFERENCES

1. Kraus, M. H., Issing, W., Miki, T., Popescu, N. C., and Aaronson, S. A. Isolation and characterization of ERBB3, a third member of the ERBB/epidermal growth factor receptor family: evidence for overexpression in a subset of human mammary tumors. Proc. Natl. Acad. Sci. USA, *86:* 9193–9197, 1989.
2. Plowman, G. D., Grenn, J. M., Culouscou, J-M., Carlton, G. W., Rothwell, V. M., and Buckley, S. Heregulin induces tyrosine phosphorylation of HER4/p180^{erbB-4}. Nature (Lond.), *366:* 473–475, 1993.
3. Ullrich, A., Coussens, L., Hayflick, J. S., Dull, T. J., Gray, A., Tam, A. W., Lee, J., Yarden, Y., Libermann, T. A., Schlessinger, J., Downward, J., Mayes, E. L. V., Whittle, N., Waterfeild, M. D., and Seeburg, P. H. Human EGF receptor cDNA sequence and aberrant expression of the amplified gene in A431 epidermoid carcinoma cells. Nature (Lond.), *309:* 418–425, 1984.
4. Yamamoto, T., Ikawa, S., Akiyama, T., Semba, K., Nomura, N., Miyajima, N., Saito, T., and Toyoshima, K. Similarity of protein encoded by the human c-*erb*B-2 gene to epidermal growth factor. Nature (Lond.), *319:* 230–234, 1986.
5. Gullick, W. J. Prevalence of aberrant expression of the epidermal growth factor receptor in human cancer cells. Br. Med. Bull., *47:* 87–98, 1991.

6. Hynes, N. E., and Stern, D. F. The biology of of erbB-2/neu/HER-2 and its role in cancer. Biochem. Biophys. Acta, *1198:* 165–184, 1994.
7. Holmes, W. E., Sliwkowski, M. X., Akita, R. W., Henzel, W. J., Lee, J., Park, J. W., Yansura, D., Abadi, N., Raab, H., Lewis, G. D., Shepard, H. M., Kuang, W-J., Wood, W. I., Goeddel, D. V., and Vandlen, R. L. Identification of heregulin, a specific activator of p185^{erbB2}. Science (Washington DC), *256:* 1205–1210, 1992.
8. Lupu, R., Colomer, R., Zugmaier, G., Sarup, J., Shepard, M., Slamon, D., and Lippman, M. E. Direct interaction of a ligand for the erbB2 oncogene product with the EGF receptor and P185 ^{erbB2}. Science (Washington DC), *249:* 1552–1555, 1990.
9. Peles, E., Bacus, S. S., Koski, R. A., Lu, H. S., Wen, D., Ogden, S. G., Ben Levy, R., and Yarden, Y. Isolation of the Neu/HER-2 stimulatory ligand: a 44 kd glycoprotein that induces differentiation of mammary tumor cells. Cell, *69:* 205–216, 1992.
10. Wen, D., Peles, E., Cupples, R., Suggs, S. V., Bacus, S. S., Luo, Y., Trail, G., Hu, S., Silbiger, S. M., Levy, R. B., Koski, R. A., Lu, H. S., and Yarden, Y. Neu differentiation factor: a transmembrane glycoprotein containing an EGF domain and an immunoglobulin homology unit. Cell, *69:* 559–572, 1992.
11. King, C. R., Borrello, I., Bellot, F., Comoglio, P., and Schlessinger, J. EGF binding to its receptor triggers a rapid tyrosine phosphorylation of the *erb*B-2 protein in the mammary tumor cell line SK-BR-3. EMBO J., *7:* 1647–1651, 1988.
12. Sliwkowski, M. X., Schaefer, G., Akita, R. W., Lofgren, J. A., Fitzpatrick, V. D., Nuijens, A., Fendly, B. M., Cerione, R. A., Vandlen, R. L., and Carraway, K. L. Coexpression of erbB2 and erbB3 proteins reconstitutes a high affinity receptor for heregulin. J. Biol. Chem., *269:* 14661–14665, 1994.
13. Bacus, S. S., Yarden, Y., Oren, M., Chin, D. M., Lyass, L., Zelnick, C. R., Kazarov, A., Toyofuku, W., Gray-Bablin, J., Beerli, R. R., Hynes, N. E., Nikiforov, M., Haffner, R., Gudkov, A., and Keyomarsi, K. Neu differentiation factor (heregulin) activates a p53-dependent pathway in cancer cells. Oncogene, *12:* 2535–2547, 1996.
14. Carraway, K. L., Soltoff, S. P., and Cantley, L. C. Heregulin stimulates mitogenesis and phosphatidylinositol 3-kinase in mouse fibroblasts transfected with erbB2/neu and erbB3. J. Biol. Chem., *270:* 7111–7116, 1995.
15. Grasso, A. W., Wen, D., Miller, C. M., Rhim, J. S., Pretlow, T. G., and Kung, H. J. ErbB kinases and NDF signaling in human prostate cancer cells. Oncogene, *15:* 2705–2716, 1997.
16. Karunagaran, D., Tzahar, E., Beerli, R. R., Chen, X., Graus-Porta, D., Ratzkin, B. J., Seger, R., Hynes, N. E., and Yarden, Y. ErbB-2 is a common auxiliary subunit of NDF and EGF receptors: implications for breast cancer. EMBO J., *15:* 254–264, 1996.
17. Marte, B. M., Jeschke, M., Graus-Porta, D., Taverna, D., Hofer, P., Groner, B., Yarden, Y., and Hynes, N. E. Neu differentiation factor/heregulin modulates growth and differentiation of HC11 mammary epithelial cells. Mol. Endocrinol., *9:* 14–23, 1995.
18. Daly, J. M., Jannot, C. B., Beerli, R. R., Graus-Porta, D., Maurer, F. G., and Hynes, N. E. Neu differentiation factor induces erbB2 down-regulation and apoptosis of erbB-2-overexpressing breast tumor cells. Cancer Res., *57:* 3804–3811, 1997.
19. Bacus, S. S., Gudkov, A. V., Zelnick, C. R., Chin, D., Stern, R., Stancovski, I., Peles, E., Ben-Baruch, N., Farbstein, H., Lupu, R., Wen, D., Sela, M., and Yarden, Y. Neu differentiation factor (heregulin) induces expression of intercellular adhesion molecule 1: implications for mammary tumors. Cancer Res., *53:* 5251–5261, 1993.
20. Staebler, A., Sommers, C., Mueller, S., Bayers, S., Thompson, E. W., and Lupu, R. Modulation of breast cancer progression and differentiation by the erbB-2 ligand (gp30). Breast Cancer Res. Treat., *31:* 175–182, 1994.
21. Adams, J. C. Cell adhesion-spreading frontiers, intricate insights. Trends Cell Biol., *7:* 107–110, 1997.
22. Gumbiner, B. M. Cell adhesion: the molecular basis of tissue architecture and morphogenesis. Cell, *84:* 345–357, 1996.
23. Royal, I., and Park, M. Hepatocyte growth factor-induced scatter of madin-darby canine kidney cells requires phosphatidylinositol 3-kinase. J. Biol. Chem., *270:* 27780–27787, 1995.
24. Guyton, K. Z., Gorospe, M., Kensler, T. W., and Holbrook, N. J. Mitogen-activated protein kinase (MAPK) activation by butylated hydroxytoluene hydroperoxide: implications for cellular survival and tumor promotion. Cancer Res., *56:* 3480–3485, 1996.
25. Xu, F-J., Stack, S., Boyer, C., O'Briant, K., Yu, Y. H., and Bast, R. C. Heregulin and agonistic anti-p185(c-erbB2) antibodies inhibit proliferation but increase invasiveness of breast cancer cells that overexpress p185(c-erbB2): increased invasiveness may contribute to poor prognosis. Clin. Cancer Res., *3:* 1629–1634, 1997.
26. Behrens, J., Mareel, M. M., Roy, F. M. V., and Birchmeier, W. Dissecting tumor cell invasion: epithelial cells acquire invasive properties after the loss of uvomorulin-mediated cell-cell adhesion. J. Cell Biol., *108:* 2435–2447, 1989.
27. Vleminck, X. K., Vakaet, J. L., Mareel, M., Fiers, W., and Roy, F. M. V. Genetic manipulation of E-cadherin expression by epithelial tumor cell reveals an invasion suppressor role. Cell, *66:* 107–119, 1991.
28. Frixen, U. H., Behrens, J., Sachs, M., Eberle, G., Voss, B., Warda, A., Lochner, D., and Birchmeier, W. E-cadherin-mediated cell-cell adhesion prevents invasiveness of human carcinoma cells. J. Cell Biol., *113:* 173–185, 1991.
29. Chen, H. C., and Guan, J. L. Association of focal adhesion kinase with its potential substrate phosphatidylinositol 3-kinase. Proc. Natl. Acad. Sci. USA, *91:* 10148–10152, 1994.
30. Alessi, D. R., Cuenda, A., Cohen, P., Dudley, D. T., and Saltiel, A. R. PD 098059 is a specific inhibitor of the activation of mitogen-activated protein kinase kinase *in vitro* and *in vivo*. J. Biol. Chem., *270:* 27489–27494, 1995.
31. Dudley, D. T., Pang, L., Decker, S. J., Bridges, A. J., and Saltiel, A. A synthetic inhibitor of the mitogen-activated protein kinase cascade. Proc. Natl. Acad. Sci. USA, *92:* 7686–7689, 1995.
32. Okada, T., Kawano, Y., Sakakibara, T., Hazeki, O., and Ui, M. Essential role of phosphatidylinositol 3-kinase in insulin-induced glucose transport and antilipolysis in rat adipocytes. Studies with a selective inhibitor wortmannin. J. Biol. Chem., *269:* 3568–3573, 1994.
33. Powis, G., Bonjouklian, R., Berggren, M. M., Gallegos, A., Abraham, R., Ashendel, C., Zalkow, L., Matter, W. F., Dodge, J., Grindey, G., and Vlahos, C. J. Wortmannin, a potent and selective inhibitor of phosphatidylinositol 3-kinase. Cancer Res., *54:* 2419–2423, 1994.
34. Vlahos, C. J., Matter, W. F., Hui, K. Y., and Brown, R. F. A specific inhibitor of phosphatidylinositol 3-kinase, 2-(4-Morpholinyl)-8-phenyl-4H–1benzopyran-4-one (LY294002). J. Biol. Chem., *269:* 5241–5248, 1994.
35. Fedi, P., Pierce, J. H., Di Fiore, P. P., and Kraus, M. H. Efficient coupling with phosphatidylinositol 3-kinase, but not phospholipase Cγ or GTPase-activating protein, distinguishes erbB-3 signaling from that of other ErbB/EGFR family members. Mol. Cell. Biol., *14:* 492–500, 1994.
36. Escobedo, J. A., Kaplan, D. R., Kavanaugh, W. M., Turck, C. W., and Williams, L. T. A phosphatidylinositol 3-kinase binds to platelet-derived growth factor receptors through a specific receptor sequence containing phosphotyrosine. Mol. Cell. Biol., *11:* 1125–1132, 1991.
37. McGlade, C. J., Ellis, C., Reedijk, M., Anderson, D., Mbamalu, G., Reith, A. D., Panayotou, G., End, P., Bernstein, A., and Kazlauskas, A. E. A. SH2 domains of the p85 α subunit of phosphatidylinositol 3-kinase regulate binding to growth factor receptors. Mol. Cell. Biol., *12:* 991–997, 1992.
38. Danilenko, D. M., Ring, B. D., Lu, J. Z., Tarpley, J. E., Chang, D., Liu, N., Wen, D., and Pierce, G. F. Neu differentiation factor upregulates epidermal migration and integrin expression in excisional wounds. J. Clin. Invest., *95:* 842–851, 1995.
39. Shaw, L. M., Rabinovitz, I., Wang, H. H. F., Toker, A., and Mercurio, A. M. Activatin of Phosphoinositide 3-OH kinase by the α6β4 integrin promotes carcinoma invasion. Cell, *91:* 949–960, 1997.
40. Frisch, S. M., and Dolter, K. E. Adenovirus E1a-mediated tumor suppression by a c-erbB-2/neu-independent mechanism. Cancer Res., *55:* 5551–5555, 1995.
41. Wennstrom, S., Siegbahn, A., Yokote, K., Arvidsson, A-K., Heldin, C-H., Mori, S., and Claesson-Welsh, L. Membrane ruffling and chemotaxis transduced by the PDGF β-receptor require the binding site for phosphatidylinositol 3-kinase. Oncogene, *9:* 651–660, 1994.
42. Hordijk, P. L., ten Klooster, J. P., van der Kammen, R. A., Michiels, F., Oomen, L. C. J. M., and Collard, J. G. Inhibition of invasion of epithelial cells by tiam 1-rac signaling. Science (Washington DC), *278:* 1464–1466, 1997.
43. Glinsky, G. V. Cell adhesion and metastasis: is the site specificity of cancer metastasis determined by leukocyte-endothelial cell recognition and adhesion? Crit. Rev. Oncol. Hematol., *14:* 229–278, 1993.
44. Raz, A. A. L., R. Endogenous-galactoside binding lectins: a new class of functional tumor cell surface molecules related to metastasis. Cancer Metastasis Rev., *6:* 433–452, 1987.
45. Fidler, I. J. The relationship of embolic homogeneity, number, size and viability to the incidence of experimental metastasis. Eur. J. of Cancer, *9:* 223–227, 1973.
46. Raz, A., Bucana, C., McLellan, W., and Fidler, I. J. Distribution of membrane anionic sites on B16 melanoma variants with differing lung colonizing potential. Nature (Lond.), *284:* 363–264, 1980.
47. Lotan, R., and Raz, A. Low colony formation *in vivo* and in culture as exhibited by metastatic melanoma cells selected for reduced homotypic aggregation. Cancer Res., *43:* 2088–2093, 1983.

Molecular Cell

Volume 2 Number 5 November 1998

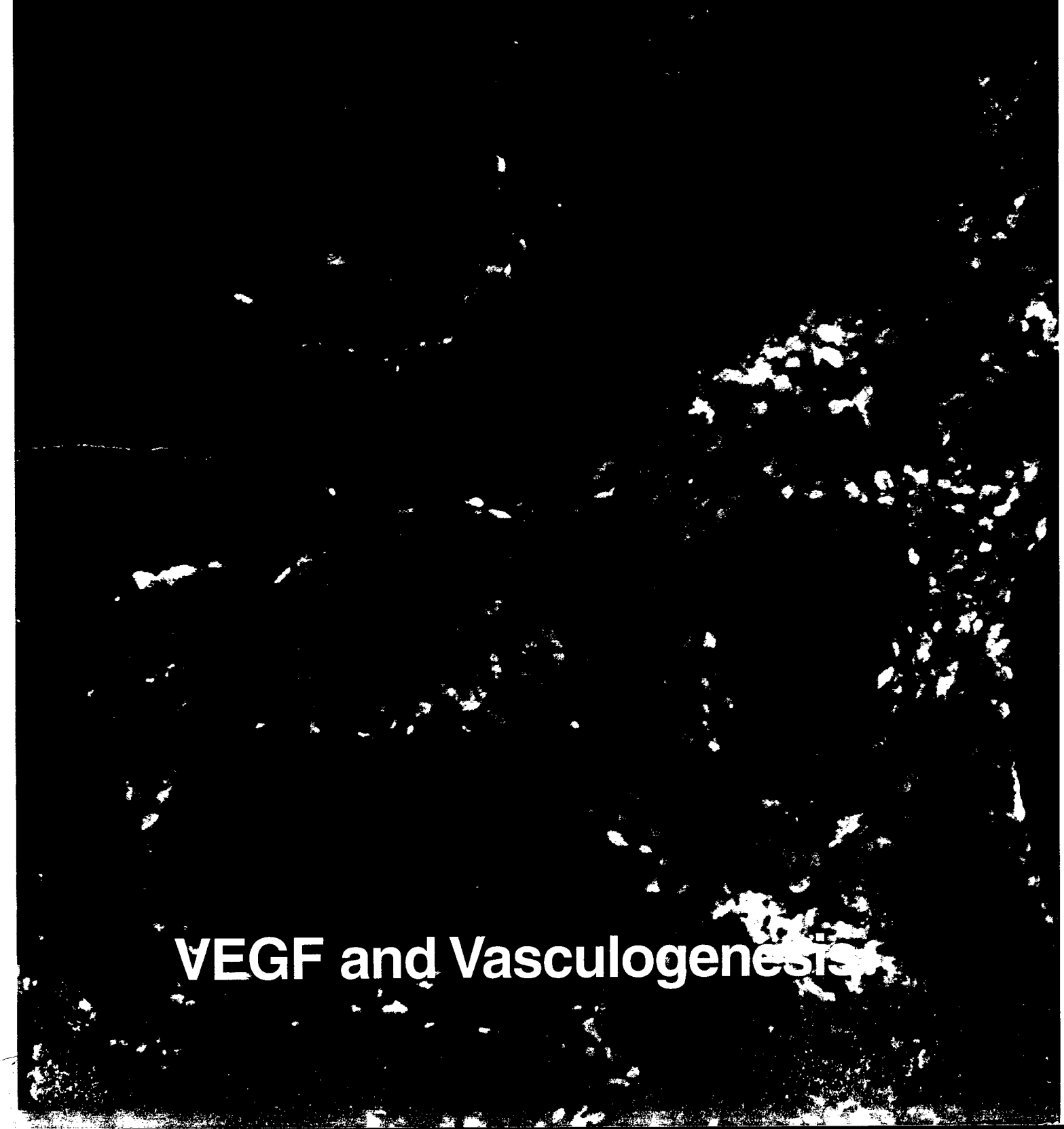

VEGF and Vasculogenesis

Molecular Cell, Vol. 2, 581–591, November, 1998, Copyright ©1998 by Cell Press

Overexpression of ErbB2 Blocks Taxol-Induced Apoptosis by Upregulation of $p21^{Cip1}$, which Inhibits $p34^{Cdc2}$ Kinase

Dihua Yu,*§ Tong Jing,* Bolin Liu,* Jun Yao,* Ming Tan,* Timothy J. McDonnell,† and Mien-Chie Hung‡
*Department of Surgical Oncology
†Department of Molecular Pathology
‡Department of Tumor Biology
The University of Texas
M. D. Anderson Cancer Center
Houston, Texas 77030

Summary

Overexpression of the receptor tyrosine kinase $p185^{ErbB2}$ confers Taxol resistance in breast cancers. Here, we investigated the underlying mechanisms and found that overexpression of $p185^{ErbB2}$ inhibits Taxol-induced apoptosis. Taxol activates $p34^{Cdc2}$ kinase in MDA-MB-435 breast cancer cells, leading to cell cycle arrest at the G2/M phase and, subsequently, apoptosis. A chemical inhibitor of $p34^{Cdc2}$ and a dominant-negative mutant of $p34^{Cdc2}$ blocked Taxol-induced apoptosis in these cells. Overexpression of $p185^{ErbB2}$ in MDA-MB-435 cells by transfection transcriptionally upregulates $p21^{Cip1}$, which associates with $p34^{Cdc2}$, inhibits Taxol-mediated $p34^{Cdc2}$ activation, delays cell entrance to G2/M phase, and thereby inhibits Taxol-induced apoptosis. In $p21^{Cip1}$ antisense-transfected MDA-MB-435 cells or in $p21^{-/-}$ MEF cells, $p185^{ErbB2}$ was unable to inhibit Taxol-induced apoptosis. Therefore, $p21^{Cip1}$ participates in the regulation of a G2/M checkpoint that contributes to resistance to Taxol-induced apoptosis in $p185^{ErbB2}$-overexpressing breast cancer cells.

Introduction

The *ErbB2* (or *HER-2*, *neu*) gene encodes a 185 kDa transmembrane glycoprotein (p185), and it was found to be amplified, overexpressed, or both in approximately 30% of human breast carcinomas (Slamon et al., 1987). Individuals with such carcinomas had a significantly lower overall survival rate and a shorter time to relapse than did patients whose tumors did not overexpress ErbB2. We previously demonstrated that ErbB2 overexpression can confer breast cancer cells increased resistance to paclitaxel (Taxol) (Yu et al., 1996). Our experimental findings are supported by recent reports from a phase III clinical trial that the response rate to Taxol was significantly improved in breast cancer patients when ErbB2 was downregulated using Herceptin antibodies that bind to the extracellular domain of ErbB2 (Dickman, 1998). However, the molecular mechanisms underlying ErbB2-mediated Taxol resistance in breast cancers were not defined.

Taxol is a potent and highly effective antineoplastic agent for the treatment of advanced, drug-refractory, metastatic breast cancers (Holmes et al., 1991). At the cellular level, Taxol induces tubulin polymerization and microtubule formation (Horwitz, 1992), blocks the cell cycle in mitosis, and induces programmed cell death (apoptosis) (Wahl et al., 1996). At the biochemical level, Taxol has been shown to increase the release of tumor necrosis factor (TNF) (Ding et al., 1990), to increase lipopolysaccharide-inducible genes and protein-tyrosine phosphorylation (Manthey et al., 1992), and to activate $p34^{Cdc2}$ inappropriately (Donaldson et al., 1994). However, the molecular pathway of Taxol-mediated cytotoxicity and apoptosis remains to be elucidated.

Apoptosis is a predominant mechanism by which cancer chemotherapeutic agents (including Taxol) kill cells (Fisher, 1994). The failure of cancer cells to detect drug-induced damage and to activate apoptosis may lead to multidrug resistance. Many intracellular signaling pathways involving growth factor receptors and their downstream signaling molecules may converge in a common apoptosis-regulatory mechanism (Collins and Rivas, 1993). Although it is known that overexpression of ErbB2 receptor confers resistance to Taxol (Yu et al., 1996), the potential impact of ErbB2 overexpression on Taxol-induced apoptosis has not been previously explored.

$p34^{Cdc2}$–cyclin B complexes are known to catalyze chromosomal condensation and nuclear envelope breakdown during mitosis. Growing evidence indicates that $p34^{Cdc2}$–cyclin B may play a role in the nuclear changes accompanying apoptosis. Activation of the $p34^{Cdc2}$ kinase at the G2/M transition is precisely controlled by multiple regulatory factors including cyclin B, Cdc25C, Myt1, Wee1, and others (for review, see Coleman and Dunphy, 1994). Interestingly, when Cdk2 kinase activity in extracts of cycling *Xenopus* eggs was inhibited by $p21^{Cip1}$, mitosis was blocked and inactive $p34^{Cdc2}$-cyclin B accumulated (Guadagno and Newport, 1996). Whether $p21^{Cip1}$ may directly inhibit $p34^{Cdc2}$ requires further investigation.

$p21^{Cip1}$ ($p21^{waf1}$, $p21^{sdi}$) encodes a 21 kDa protein and was discovered as a Cdk inhibitor (Harper et al., 1993) as well as a wild-type p53-inducible gene (El-Deiry et al., 1993). Later, $p21^{Cip1}$ was considered critical for the coordination of the S and M phases of the cell cycle, because doxorubicin-treated $p21^{-/-}$ cancer cells but not parental $p21^{+/+}$ cells experienced multiple rounds of S phase without mitosis and then became apoptotic (Waldman et al., 1996). Although $p21^{Cip1}$ has recently been shown to contribute to regulation of the G2/M transition (Dulic et al., 1998), the biological impact of such regulation when cells suffer DNA damage or disorder in mitosis (e.g., exposure to Taxol) has not been clearly demonstrated.

In an attempt to understand the molecular mechanisms underlying ErbB2-mediated Taxol resistance, we conducted the current study and found that ErbB2 blocks Taxol-induced apoptosis in breast cancer cells by upregulation of $p21^{Cip1}$, which participates in the negative regulation of Taxol-mediated $p34^{Cdc2}$ activation required for Taxol-induced apoptosis. We provide experimental evidence for the role of $p21^{Cip1}$ in the regulation of G2/M checkpoint and the impact of such regulation on Taxol-mediated apoptosis in breast cancer cells. This

§To whom correspondence should be addressed.

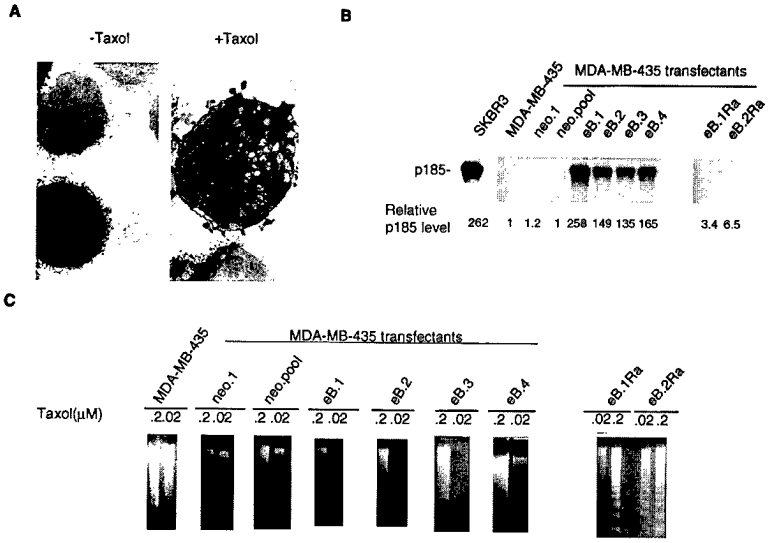

Figure 1. Overexpression of p185^{ErbB2} Inhibited Taxol-Mediated Apoptosis

(A) Morphology of MDA-MB-435 cells cultured in media without or with 0.02 μM Taxol for 24 hr under transmission electronmicroscopy (TEM). Magnification of the originals was 2000×.

(B) Western blot analysis of p185^{ErbB2} in the indicated cell lines. The relative p185 levels represent the amount of p185 in each cell line as fold of that of the MDA-MB-435 cells and were determined by quantitation with the Personal Densitometer 50371 (Molecular Dynamics, Sunnyvale, CA).

(C) DNA fragmentation assays showing that overexpression of p185^{ErbB2} in MDA-MB-435 transfectants inhibited Taxol-induced apoptosis. The low molecular weight DNAs were isolated from the indicated cell lines cultured in media containing indicated concentrations of Taxol (0.02 or 0.2 μM) and processed for DNA fragmentation assays.

study has revealed a plausible molecular mechanism underlying the Taxol resistance phenomenon in breast cancers and potentially other cancer types that overexpress ErbB2.

Results

Breast Cancer Cells Overexpressing p185^{ErbB2} Are More Resistant to Taxol-Induced Apoptosis

The MDA-MB-435 human breast cancer cell line contains only one copy of the *ErbB2* gene per haploid, expresses low levels of p185^{ErbB2} protein, and is highly sensitive to Taxol cytotoxicity (Yu et al., 1996). To investigate whether Taxol elicited cytotoxicity by induction of apoptosis, untreated and Taxol-treated MDA-MB-435 cells were examined for apoptotic morphology using light microscopy and transmission electronmicroscopy (TEM). Dramatic morphological changes specific to apoptotic cells (e.g., chromatin condensation, formation of membrane-bound apoptotic bodies, etc.) were observed in Taxol-treated cells but not in the untreated cells (Figure 1A). We also detected DNA fragmentation in Taxol-treated MDA-MB-435 cells (Figure 1C). Thus, induction of apoptosis is an important mechanism underlying the cytotoxic effects of Taxol on these breast cancer cells.

To study whether p185^{ErbB2} overexpression may confer Taxol resistance by blocking Taxol-induced apoptosis, we used a panel of cell lines with the same genetic background but expressing different levels of p185^{ErbB2} (Figure 1B). The 435.eB transfectants (eB1, eB2, eB3, and eB4) were generated by transfecting MDA-MB-435 cells with the pCMVerbB2 plasmid containing the full-length normal human *ErbB2* cDNA, and they express p185^{ErbB2} at 258-, 149-, 135-, and 165-fold, respectively, that of the parental MDA-MB-435 cells (Yu et al., 1996). The p185^{ErbB2} levels in these 435.eB transfectants are comparable to, or lower than, that in the SKBR3 breast cancer cells established from a different primary breast tumor, which express p185^{ErbB2} at 262-fold of that of the MDA-MB-435 cells (Yu et al., 1996). The control 435.neo.1 and 435.neo.pool cell lines were established by transfecting the neomycine resistance gene pSV2-*neo* alone into MDA-MB-435 cells, and they express p185^{ErbB2} at levels similar to that of the MDA-MB-435 cells (Yu et al., 1996). The eB.1Ra and eB.2Ra are two spontaneous revertants derived from the 435.eB1 and 435.eB2 that lost the transfected *ErbB2* gene and do not overexpress p185^{ErbB2} anymore. These cell lines that express different levels of p185^{ErbB2} were assayed for susceptibility to Taxol-induced apoptosis by DNA fragmentation assays (Figure 1C). Taxol-treated MDA-MB-435, 435.neo, and 435.neo.pool cells (0.02 μM) formed DNA ladders, whereas DNA ladder formation was inhibited in all four of the 435.eB transfectants. DNA ladders in 435.eB transfectants appeared only when a 10-fold higher concentration of Taxol was added. The eB.1Ra and eB.2Ra revertants demonstrated DNA ladders similar to that of the parental MDA-MB-435 cells, that is, these revertants have lost the apoptosis-resistant phenotype of the 435.eB1 and 435.eB2 cells due to the loss of p185 expression. The results indicate that overexpression of p185^{ErbB2} in breast cancer cells can inhibit Taxol-induced apoptosis.

Taxol Induces Apoptosis at the G2/M Phase of the Cell Cycle, which Is Impeded by Overexpression of p185^{ErbB2}

Taxol was previously shown to induce phosphorylation of Bcl-2, thereby inactivating Bcl-2 and inducing apoptosis in several cancer types (Blagosklonny et al., 1996). Phosphorylated Bcl-2 proteins can be detected as slower migrating bands in Western blots. No significant difference in Bcl-2 protein levels or Bcl-2 phosphorylation was observed between Taxol-treated, apoptosis-sensitive MDA-MB-435 cells and apoptosis-resistant 435.eB transfectants by Western blot analysis using Bcl-2 antibody (Figure 2A). Therefore, inhibition of Taxol-induced apoptosis by p185^{ErbB2} was unlikely to be the result of increased Bcl-2 activity.

It has been recognized that the position of cells in the cell cycle may play a role in determining susceptibility to apoptosis in many cell types (Meikrantz and Schlegel, 1996). To explore the mechanisms of Taxol-induced

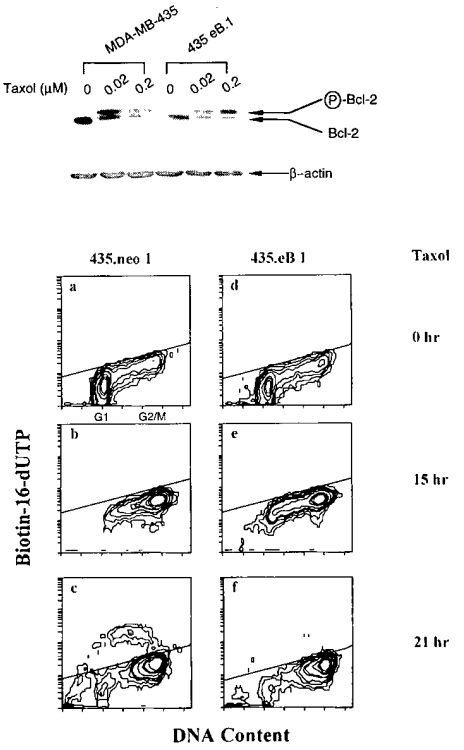

Figure 2. p185^{ErbB2} Inhibits Taxol-Induced Apoptosis by Delaying Cell Entrance to G2/M Phase of the Cell Cycle but Not by Increasing Bcl-2

(A) Bcl-2 protein levels and induction of Bcl-2 phosphorylation are similar between MDA-MB-435 and 435.eB cells. Immunoblot analysis of the Bcl-2 proteins in the cell lysates of the MDA-MB-435 cells and 435.eB1 transfectants treated with Taxol-free media (0) or with media containing the indicated concentrations of Taxol (0.02, 0.2) was performed using an antibody against human Bcl-2. Positions of the phosphorylated [(p)-Bcl-2] and nonphosphorylated Bcl-2 (Bcl-2) are indicated on the right. Immunoblotting of β-actin was used as the protein loading control.

(B) Taxol induces apoptosis at the G2/M phase of the cell cycle, which is inhibited by p185^{ErbB2}. The 435.neo and 435.eB1 transfectants were treated with 0.02 μM Taxol for 0, 15, or 21 hr and were harvested for double-label flow cytometry analyses. Apoptotic cells with DNA strand breaks are shown to have higher levels of biotin-16-dUTP labeling above the sloped lines, which were placed based on the biotin-16-dUTP signal levels in the control cells without Taxol.

apoptosis and p185^{ErbB2}-mediated antiapoptosis, we examined the cell cycle stage or stages where Taxol induced apoptosis by multiparameter flow cytometry. Cell cycle stage and apoptosis were simultaneously determined by measuring DNA content and by labeling DNA strand breaks with biotinylated dUTP (Darzynkiewicz et al., 1992). Flow cytometric analysis demonstrated that the majority of the untreated 435.neo control cells were at the G1 phase of the cell cycle without significant DNA strand breaks (Figure 2Ba). After 15 hr of 0.02 μM Taxol treatment, 72% of these p185-low-expressing cells progressed to the G2/M phase (Figure 2Bb). After 21 hr of Taxol treatment, more of these cells were arrested at the G2/M phase, and some of these cells were at the sub-G1 phase indicative of apoptosis (Figure 2Bc). That the 435.neo cells were arrested at G2/M by Taxol seems to be an abortive event, since 21% of cells died at the G2/M phase as demonstrated by a high-level dUTP labeling indicating apoptotic DNA strand breaks (Figure 2Bc, over the sloped line). In contrast, the Taxol-resistant 435.eB1 cells progressed less effectively toward the G2/M phase after 15 hr of Taxol treatment (55%, Figure 2Be) and demonstrated minimal apoptotic DNA strand breaks (5%) after 21 hr of Taxol treatment (Figure 2Bf), despite untreated 435.eB cells showing a similar cell cycle distribution profile to that of the untreated 435.neo cells (Figure 2Bd). These results indicate that Taxol-induced apoptosis of the 435.neo cells occurs preferentially at the G2/M phase of the cell cycle, whereas overexpression of p185^{ErbB2} in 435.eB cells delays Taxol-mediated cell entrance to the G2/M phase, thereby inhibiting Taxol-induced apoptosis.

Taxol Induces G2/M Arrest and Apoptosis by Activation of p34^{Cdc2}–Cyclin B Kinase

Entry to mitosis is delicately controlled by the Cdk–cyclin complex consisting of the p34^{Cdc2} protein kinase and cyclin B (Draetta et al., 1989). Here, we show that Taxol can activate the p34^{Cdc2}–cyclin B1 kinase in MDA-MB-435 breast cancer cells (Figures 3A and 3C, lane 1 versus lane 4), which correlated with the induction of apoptosis at the G2/M phase (Figure 3Db). To determine whether the activation of p34^{Cdc2}–cyclin B1 kinase was required for Taxol-induced apoptosis, we investigated the effects of inhibiting p34^{Cdc2} kinase on Taxol-induced apoptosis by two approaches. First, we examined the effects of olomoucine, a potent chemical inhibitor of p34^{Cdc2}, on Taxol-induced apoptosis. MDA-MB-435 cells were cultured for 24 hr in Taxol-free media or Taxol-containing media with the addition of isoolomoucine (a control chemical) or olomoucine, respectively. The differently treated cells were then assayed for the p34^{Cdc2} kinase activities and apoptotic cell death. Olomoucine, but not isoolomoucine, reduced (30%) Taxol-mediated activation of p34^{Cdc2} (Figure 3A). Parallel to the inhibition of p34^{Cdc2} kinase activity, olomoucine effectively inhibited Taxol-induced apoptosis, since flow cytometry demonstrated that MDA-MB-435 cells treated with olomoucine plus Taxol had dramatically reduced sub-G1 apoptotic cells compared with cells treated with Taxol alone or with isoolomoucine plus Taxol (Figure 3B).

Since olomoucine functions by competing for the ATP binding domain of the kinase and may have weak inhibitory effects on other Cdks (Vesely et al., 1994), our second approach was to specifically inhibit p34^{Cdc2} using the dominant-negative mutant of p34^{Cdc2}, pCMVcdc2-dn (van den Heuvel and Harlow, 1993). MDA-MB-435 cells were transfected with the pCMVcdc2-dn, or pCMVneo for 36 hr, then cultured with or without Taxol for an additional 21 hr and harvested. RNA expression from the transfected Cdc2-dn was detected by RT-PCR using PCR primers that specifically amplify Cdc2-dn (Figure 3G). Taxol-mediated activation of p34^{Cdc2} was reduced in the pCMVcdc2-dn-transfected cells (76% reduction), whereas no discernible inhibitory effect was observed in the pCMVneo-transfected cells (Figure 3C). Meanwhile, Cdc2-dn retarded Taxol-induced cell progression to

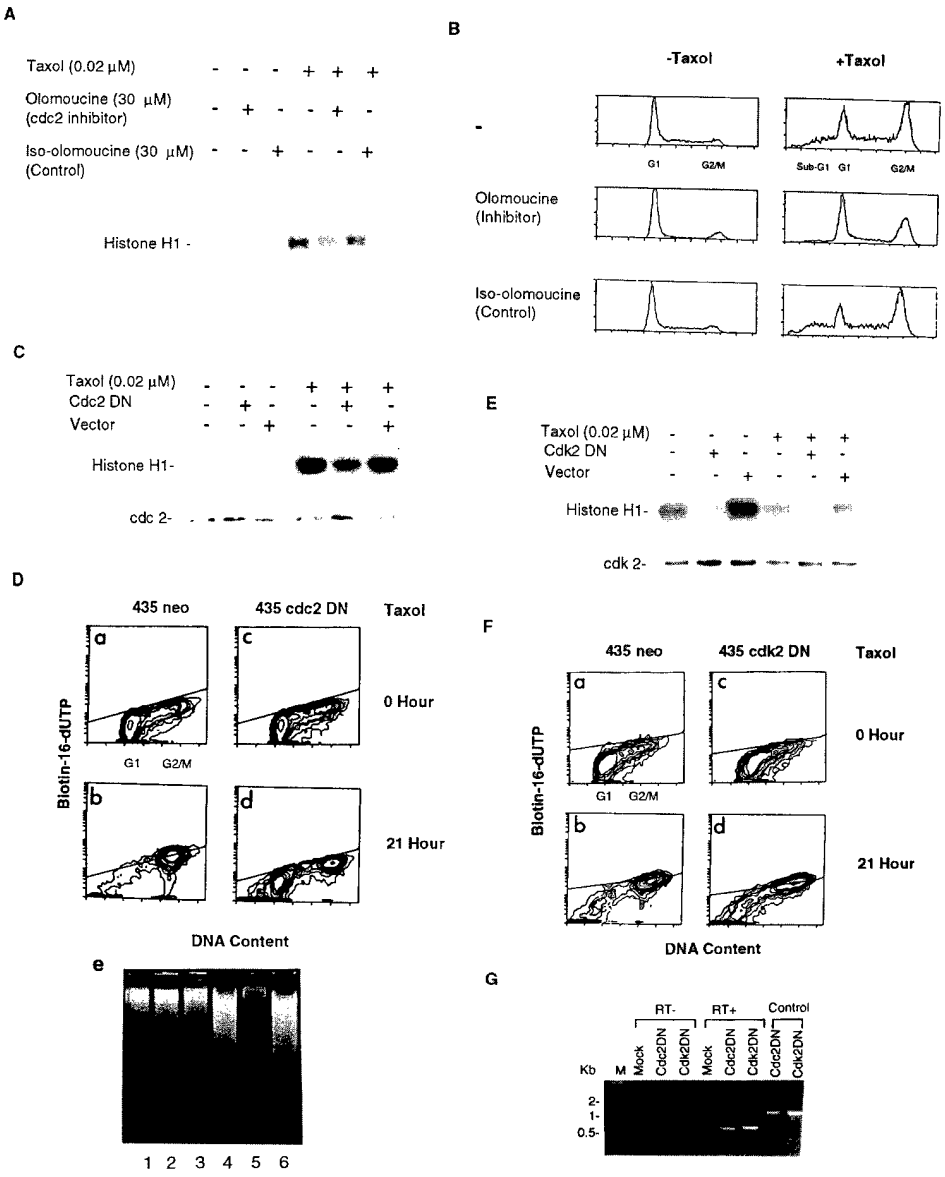

Figure 3. Activation of p34^{Cdc2} Kinase Is Required for Taxol-Mediated Apoptosis

(A) Inhibition of p34^{Cdc2} kinase activity by olomoucine. MDA-MB-435 cells were cultured for 24 hr in Taxol-free media, or Taxol-containing media (0.02 μM), alone, with addition of isoolomoucine, or with olomoucine. These differently treated cells were then assayed for p34^{Cdc2} kinase activities by determining their ability to phosphorylate histone H1 substrate.

(B) Olomoucine inhibited Taxol-induced apoptosis. MDA-MB-435 cells treated in a similar manner as in Figure 3A were collected and stained with propidium iodide for flow cytometric analysis. Apoptosis was represented by the appearance of cells at the sub-G1 phase.

(C) Inhibition of p34^{Cdc2} kinase activity by the dominant-negative mutant of p34^{Cdc2} (Cdc2-dn). MDA-MB-435 cells were mock transfected or transfected with pCMVneo vector, or with pCMVcdc2-dn using cationic liposome, DC-Chol:DOPE. Thirty-six hours later, cells were grown in fresh media with (0.02 μM) or without Taxol for another 21 hr. These differently treated cells were then harvested and assayed for p34^{Cdc2} kinase activities as in (A). The p34^{Cdc2} protein levels were determined by Western blot analysis using anti-Cdc2 antibodies (bottom). Activation of p34^{Cdc2} kinase activities was reduced (76.2% reduction after normalized with Cdc2 protein level) in the Cdc2-dn-transfected cells compared to that in mock-transfected cells.

(D) Inhibition of Taxol-induced apoptosis by Cdc2-dn. Cells treated in a similar manner as in (C) were collected and detected for Taxol-induced apoptosis by double-label flow cytometry analysis (a–d) and by DNA fragmentation assay (e, lanes 1–6 correspond to lanes 1–6 in [C]).

(E) Inhibition of Cdk2 kinase activity by the dominant-negative mutant of Cdk2 (Cdk2-dn). MDA-MB-435 cells were treated and assayed in a similar manner as in (C) except pCMVcdk2-dn was used here.

(F) Cdk2-dn did not inhibit Taxol-induced apoptosis. MDA-MB-435 cells were treated and assayed in a similar manner as described in (D) except pCMVcdk2-dn was used here.

(G) RNA expression of the transfected pCMVcdc2-dn and pCMVcdk2-dn.

MDA-MB-435 cells were mock transfected, transfected with pCMVcdc2-dn or pCMVcdk2-dn for 36 hr, and processed for RT-PCR experiments. RT−, PCR without reverse transcription; RT+, reverse transcription followed by PCR; control, direct PCR using pCMVcdc2-dn and pCMVcdk2-dn plasmids as PCR template, which yielded signals ~600 bp larger than that from RNA transcripts. This was due to the β-globin intron 2 sequence existing in both plasmids.

G2/M phase and dramatically reduced apoptosis compared with pCMVneo-transfected cells that were effectively blocked at the G2/M phase by Taxol and underwent apoptosis (Figure 3Dd versus 3Db). Inhibition of Taxol-induced apoptosis by Cdc2-dn in MDA-MB-435 cells was also observed using DNA fragmentation assays (Figure 3De, lane 5 versus 4). Blocking of Taxol-induced apoptosis by inhibition of p34^{Cdc2} with olomoucine and Cdc2-dn indicated that activation of p34^{Cdc2} was required for Taxol-induced apoptosis.

Cdk2 was previously shown to be required for entry into mitosis as a positive regulator of p34^{Cdc2} kinase in extracts of cycling *Xenopus* eggs (Guadagno and Newport, 1996). We next investigated whether Cdk2 is required for Taxol-mediated entrance of MDA-MB-435 cells to G2/M phase and apoptosis using the dominant-negative mutant of Cdk2, pCMVcdk2-dn (van den Heuvel and Harlow, 1993). MDA-MB-435 cells were transfected with the pCMVcdk2-dn, or CMV vector for 36 hr, then cultured in the presence or absence of Taxol for an additional 21 hr and harvested. RNA expression from the transfected Cdk2-dn was also detected by RT-PCR (Figure 3G). Interestingly, Taxol did not activate Cdk2 kinase activity in MDA-MB-435 cells (Figure 3E, lane 1 versus lane 4), suggesting that Taxol did not induce apoptosis by activating Cdk2. Additionally, Cdk2-dn did not block Taxol-induced apoptosis in these cells (Figure 3Fd), although Cdk2-dn effectively inhibited the kinase activities of Cdk2 (Figure 3E), indicating that Cdk2 is not required for Taxol-induced apoptosis. Similarly, Cdk4 was found not necessary for Taxol-induced apoptosis in MDA-MB-435 cells (data not shown) using dominant-negative Cdk4 mutant pCMVcdk4-dn (van den Heuvel and Harlow, 1993). Taken together, activated p34^{Cdc2}, but not Cdk2 or Cdk4, is one of the mediators for Taxol-induced apoptosis.

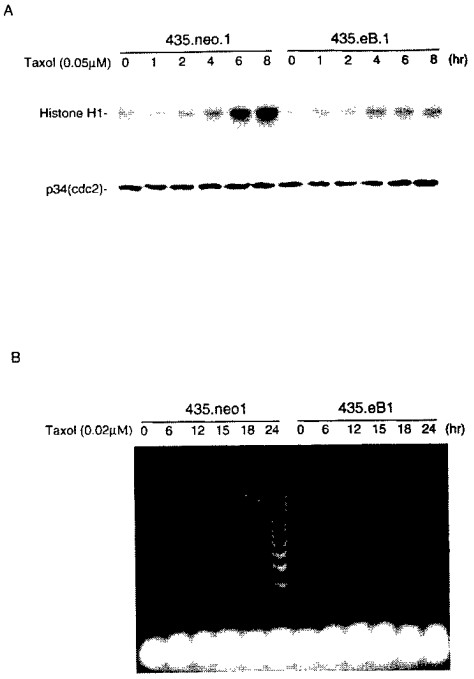

Figure 4. Taxol-Induced Activation of p34^{Cdc2} and Apoptosis Are Inhibited in p185-Overexpressing 435.eB1 Cells

(A) Taxol-mediated p34^{Cdc2} activation is inhibited in 435.eB1 cells. Protein lysates from either 435.neo1 or 435.eB1 cells were collected at the indicated time points after addition of 0.05 μM Taxol. Equal amounts of protein lysates were immunoprecipitated using the anti-Cdc2 antibodies, and immunocomplexes were subjected to kinase assays. Cdc2 protein levels were determined by Western blotting using anti-Cdc2 antibodies.

(B) Taxol-induced apoptosis is delayed and reduced in 435.eB1 cells compared with that in 435.neo1 cells. The low molecular weight DNA was isolated from either 435.neo1 or 435.eB1 cells at the indicated time points after addition of 0.02 μM Taxol and processed for DNA fragmentation assays.

Taxol-Induced Activation of p34^{Cdc2} Is Inhibited in 435.eB Cells

To examine whether overexpression of p185^{ErbB2} may inhibit Taxol-mediated activation of p34^{Cdc2} and thereby confer resistance to Taxol-induced apoptosis, we compared the extent and kinetics of Taxol-induced activation of p34^{Cdc2} kinase between the p185^{ErbB2}-low-expressing 435.neo cells and the p185^{ErbB2}-overexpressing 435.eB transfectants. Activation of p34^{Cdc2} kinase in 435.neo cells was detected 2 hr after addition of Taxol, and it continued to increase 8 hr after Taxol treatment compared to that in the untreated cells (Figure 4A). However, activation of p34^{Cdc2} kinase in the Taxol-resistant 435.eB cells is reduced to only 47% of that in the 435.neo cells (Figure 4A), whereas the p34^{Cdc2} protein levels are similar between the 435.neo cells and 435.eB cells (Figure 4A, bottom). To investigate whether the inhibition of p34^{Cdc2} activation by p185^{ErbB2} may contribute to resistance to Taxol-induced apoptosis, 435.neo cells and 435.eB cells were compared for the kinetics of Taxol-induced apoptosis using DNA fragmentation assays (Figure 4B). DNA ladders appeared in the 435.neo cells 12 hr after 0.02 μM Taxol treatment and became pronounced 15 hr after Taxol treatment. However, DNA ladders in the 435.eB cells did not appear until 18 hr after Taxol treatment, and the degree of DNA fragmentation was less pronounced than that in 435.neo cells. The delayed and reduced apoptotic response in the Taxol-treated 435.eB cells correlated with their lower p34^{Cdc2} kinase activity, suggesting that inhibition of Taxol-mediated p34^{Cdc2} activation in 435.eB cells may contribute to their resistance to Taxol-induced apoptosis.

Elevated p21^{Cip1} Expression in 435.eB Transfectants

It is known that activation of p34^{Cdc2} is precisely regulated by the accumulation of cyclin B and by three phosphorylation sites on the p34^{Cdc2} subunit that are modulated by Cdc25 and Wee1. To determine how p185^{ErbB2} inhibited the activation of p34^{Cdc2}, we compared the expression levels of these p34^{Cdc2} regulators in the p185-low-expressing 435.neo cells and p185-overexpressing 435.eB cells by immunoblot analysis, and no significant difference was detected among these cells (data not shown). This suggests that overexpression of p185^{ErbB2} did not inhibit activation of p34^{Cdc2} by regulating cyclin B, Cdc25, and Wee1 expression.

In addition to these regulators of p34^{Cdc2}, p21^{Cip1} was suggested to regulate a G2/M checkpoint, blocking the entrance of cells into M phase (Jacks and Weinberg,

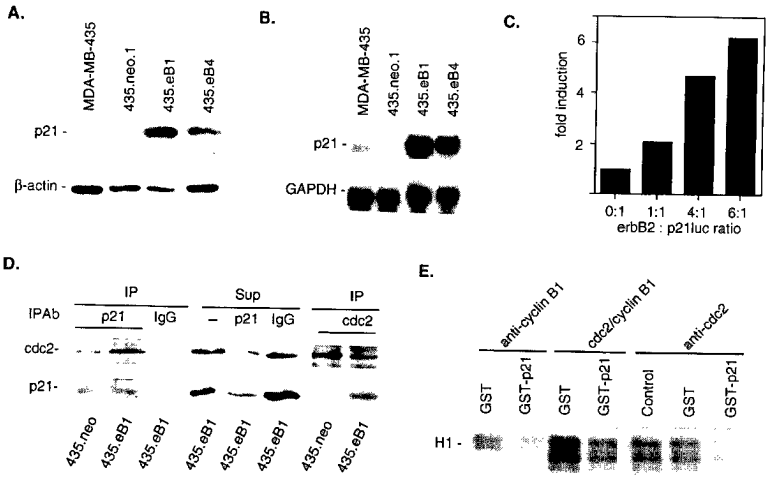

Figure 5. $p185^{ErbB2}$ Upregulates $p21^{Cip1}$, which Inhibits $p34^{Cdc2}$

(A) $p21^{Cip1}$ protein levels are higher in the $p185^{ErbB2}$-overexpressing 435.eB transfectants than in the parental MDA-MB-435 and control 435.neo.1 cells. Immunoblot analyses were performed using the $p21^{Cip1}$ antibody (top) or the β-actin antibody as a control (bottom).

(B) Northern blot analysis demonstrated higher steady-state *$p21^{Cip1}$* mRNA levels in the $p185^{ErbB2}$-overexpressing 435.eB transfectants than in the control cells. RNA blot was hybridized with a ^{32}P-labeled cDNA probe of $p21^{Cip1}$ (top) or GAPDH as a control (bottom).

(C) ErbB2 transcriptionally upregulated $p21^{Cip1}$. MDA-MB-435 cells (1×10^6) in 60 mm dishes were cotransfected using cationic liposome with 1.5 μg pCMV-lacZ, 1 μg pWWP-Luc, and different concentrations of pCMVerbB2 resulting in the pCMVerbB2 to pWWP-Luc (ErbB2: p21luc) ratios of 0:1, 1:1, 4:1, and 6:1. The total amount of transfected DNA was brought up to 9 μg by adding pCMVneo. Luciferase activities were measured 40 hr after transfection and were standardized by transfection efficiency.

(D) Association of $p21^{Cip1}$ with $p34^{Cdc2}$. Cell lysates were prepared from 435.neo and 435.eB1 cell lines. Total protein (500 μg) was immunoprecipitated with antibodies against $p21^{Cip1}$ or $p34^{Cdc2}$. Immunoprecipitates (IP) and 80 μg of the supernatants (Sup) were resolved on 12% SDS-PAGE, and associated $p21^{Cip1}$ and $p34^{Cdc2}$ proteins were analyzed by immunoblotting. Normal mouse and rabbit IgG were used as controls.

(E) Recombinant $p21^{Cip1}$ protein directly inhibited $p34^{Cdc2}$–cyclin B1 kinase activity. Protein lysates from MDA-MB-435 cells were collected and immunoprecipitated using the anti-cyclin B1 antibody. Equal amounts of the immunocomplexes or equal amounts of the recombinant $p34^{Cdc2}$–cyclin B1 proteins were then subjected to kinase assays with 10 μg of recombinant GST or GST-$p21^{Cip1}$ proteins. As controls, protein lysates from MDA-MB-435 cells were also immunoprecipitated using the anti-Cdk2 antibody and subjected to kinase assays without (control) or with 10 μg of recombinant GST or GST-$p21^{Cip1}$ proteins.

1996). To investigate whether $p185^{ErbB2}$ may inhibit $p34^{Cdc2}$ kinase activity by upregulation of $p21^{Cip1}$, we examined the $p21^{Cip1}$ expression levels in MDA-MB-435 cells and 435.neo cells that express low levels of $p185^{ErbB2}$ and in 435.eB transfectants that express high levels of $p185^{ErbB2}$. Higher levels of $p21^{Cip1}$ protein were detected in the 435.eB transfectants compared with MDA-MB-435 and 435.neo control cells (Figure 5A), which was due to upregulation of $p21^{Cip1}$ mRNA expression (Figure 5B). To further investigate whether $p185^{ErbB2}$ upregulated $p21^{Cip1}$ by transcriptional activation, we cotransfected into MDA-MB-435 cells the pWWP-Luc plasmid, containing 2.4 kb wild-type *$p21^{Cip1}$* promoter and upstream sequences fused with the luciferase reporter gene (El-Deiry et al., 1993), with either the pCMVneo control vector or with increasing amounts of the pCMVerbB2, an ErbB2 expression vector (Yu et al., 1996). Luciferase activities driven by the *$p21^{Cip1}$* promoter increased in the presence of ErbB2 expression vector in an ErbB2 concentration–dependent manner (Figure 5C). These data demonstrated that $p185^{ErbB2}$ can upregulate $p21^{Cip1}$ in 435.eB transfectants at the transcriptional level.

$p21^{Cip1}$ Associates with $p34^{Cdc2}$ and Inhibits $p34^{Cdc2}$ Kinase Activity

Although $p185^{ErbB2}$ upregulated $p21^{Cip1}$ expression in 435.eB cells and $p21^{Cip1}$ was shown to regulate the G2/M transition (Dulic et al., 1998; Niculescu et al., 1998), it is not clear whether the upregulated $p21^{Cip1}$ in 435.eB cells may inhibit $p34^{Cdc2}$ and mediate the antiapoptotic function of $p185^{ErbB2}$. We therefore examined whether the upregulated $p21^{Cip1}$ in 435.eB cells may associate with $p34^{Cdc2}$ in vivo. The 435.neo and 435.eB1 cell lysates were immunoprecipitated using $p21^{Cip1}$ antibodies or control IgG. Immunoprecipitates (IP) and supernatants (Sup) were separated on SDS-PAGE and immunoblotted with antibodies against $p34^{Cdc2}$ and $p21^{Cip1}$. Abundant $p34^{Cdc2}$ protein was detected in the 435.eB1 cell precipitates of $p21^{Cip1}$ antibodies (Figure 5D, left panel), whereas little $p34^{Cdc2}$ protein remained in the supernatant due to depletion of $p21^{Cip1}$ (Figure 5D, middle panel). In addition, a stronger $p34^{Cdc2}$ signal can be detected in the 435.eB1 cells expressing high levels of $p21^{Cip1}$ compared with the 435.neo cells expressing low levels of $p21^{Cip1}$ (Figure 5D, left panel). Reverse experiments detected $p21^{Cip1}$ in the $p34^{Cdc2}$ antibody immunoprecipitates (Figure 5D, right panel). These results indicate that the upregulated $p21^{Cip1}$ protein in 435.eB cells physically associates with $p34^{Cdc2}$, suggesting that upregulation of $p21^{Cip1}$ may contribute to inactivation of $p34^{Cdc2}$ kinase in 435.eB cells.

To examine whether $p21^{Cip1}$ can indeed inhibit $p34^{Cdc2}$, we tested the inhibitory effects of purified recombinant GST-$p21^{Cip1}$ fusion protein (El-Deiry et al., 1993) on $p34^{Cdc2}$–cyclin B1 kinase activity. $p34^{Cdc2}$-cyclin B1 complexes were immunoprecipitated by anti-cyclin B1 antibodies, and Cdk2-cyclin complexes were immunoprecipitated by anti-Cdk2 antibodies (as a positive control) from MDA-MB-435 total cell lysates. The immunoprecipitates were incubated with GST-$p21^{Cip1}$ or control GST protein and then assayed for kinase activity. GST-$p21^{Cip1}$ effectively inhibited the G2/M phase $p34^{Cdc2}$–cyclin B1 kinase activity (Figure 5E, left panel). Since GST-$p21^{Cip1}$ could inhibit activities of $p34^{Cdc2}$–cyclin B1 complexes precipitated by anti-cyclin B1 antibodies, the data indicated that $p21^{Cip1}$ inhibited the $p34^{Cdc2}$ kinases that were active in the mitosis-promoting $p34^{Cdc2}$–cyclin B1 heterodimer. In the control experiment, GST-$p21^{Cip1}$ inhibited Cdk2 activity as expected (Figure 5E, right panel). Furthermore, the purified GST-$p21^{Cip1}$ fusion protein also

inhibited the activities of the purified recombinant p34^{Cdc2}–cyclin B1 kinases (Figure 5E, middle panel). Therefore, p21^{Cip1} can directly inhibit p34^{Cdc2}–cyclin B1 kinase activity in vitro.

Sensitization of 435.eB Cells to Taxol-Induced Activation of p34^{Cdc2} and Apoptosis by Antisense p21^{Cip1}

To investigate whether the upregulated p21^{Cip1} in p185^{ErbB2}-overexpressing 435.eB cells may inhibit Taxol-mediated activation of p34^{Cdc2} kinase, thereby blocking Taxol-induced apoptosis in these cells, we blocked *p21^{Cip1}* mRNA expression in 435.eB cells by transient transfection of p21^{Cip1} antisense oligonucleotides (P21AS) that hybridize to the transcription initiation site. In the control experiment, the 435.eB cells were transfected with scrambled p21^{Cip1} antisense oligonucleotide (P21S). Thirty-six hours after transfection, the 435.eB cells were treated with or without Taxol for an additional 21 hr and cell lysates harvested. Western blot analysis using p21^{Cip1} antibodies demonstrated that the p21^{Cip1} scrambled oligonucleotide-treated 435.eB cells expressed readily detectable p21^{Cip1} protein, and the p21^{Cip1} protein was slightly upregulated by Taxol (Figure 6A), which is consistent with previous reports that Taxol can induce p21^{Cip1} in certain cell types (Barboule et al., 1997). However, p21^{Cip1} antisense-treated 435.eB cells had significantly reduced p21^{Cip1} protein levels, and Taxol did not upregulate p21^{Cip1} in these cells. Higher p34^{Cdc2} kinase activity was detected in Taxol-treated 435.eB cells transfected with p21^{Cip1} antisense compared with those transfected with the scrambled oligonucleotides (Figure 6B), whereas the p34^{Cdc2} protein levels remained similar. These experiments suggest that p21^{Cip1} contributes to inhibition of Taxol-induced p34^{Cdc2} activation in 435.eB cells. We next compared the induction of apoptosis by Taxol in the antisense or scrambled oligonucleotide-transfected 435.eB cells using flow cytometry (Figure 6C). The majority of the untreated 435.eB cells with scrambled oligonucleotide were at the G1 phase of the cell cycle without significant apoptotic DNA strand breaks (Figure 6C, top panel, 0 hr). After Taxol treatment for 15 hr and 21 hr, these cells cycled toward the G2/M phase of the cell cycle with no significant DNA strand breaks (Figure 6C). Although the untreated 435.eB cells with antisense p21^{Cip1} had similar cell cycle profiles (Figure 6C, bottom panel, 0 hr) as the control cells, these cells showed a high level of apoptotic DNA strand breaks after 15 hr of Taxol treatment that became more pronounced after 21 hr of Taxol treatment (Figure 6C). Since blocking of p21^{Cip1} by antisense in 435.eB cells relieved the inhibition of Taxol-mediated p34^{Cdc2} activation and sensitized the 435.eB cells to Taxol-induced apoptosis, the data indicate that upregulated p21^{Cip1} in 435.eB transfectants participated in the inhibition of Taxol-mediated p34^{Cdc2} activation, which contributes to resistance to Taxol-induced apoptosis.

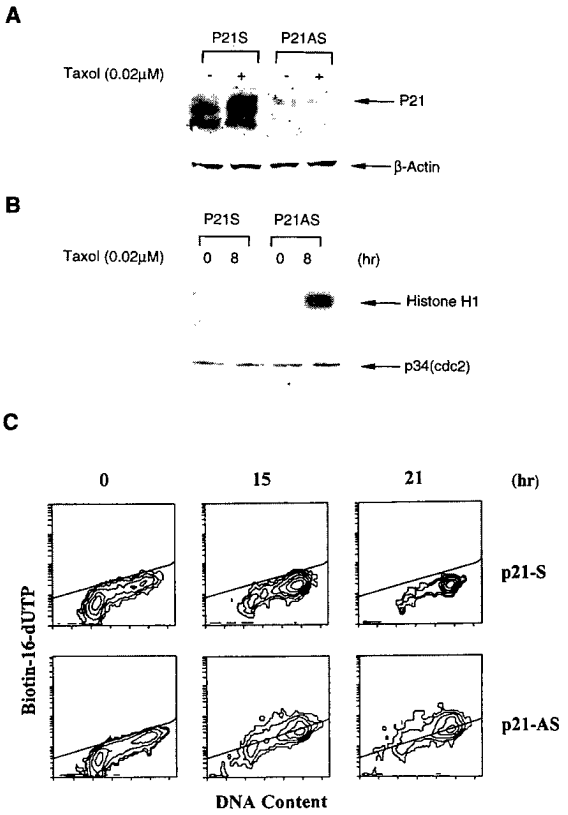

Figure 6. Antisense p21^{Cip1} Sensitized 435.eB Cells to Taxol-Induced Activation of p34^{Cdc2} and Apoptosis

(A) Transfection of p21^{Cip1} antisense oligonucleotide reduced p21^{Cip1} protein levels. The 435.eB cells were transfected with p21^{Cip1} antisense oligonucleotide (P21AS) or scrambled p21^{Cip1} antisense oligonucleotide (P21S) as a control. Thirty-six hours later, the cells were cultured in the absence (−) or presence (+) of 0.02 μM Taxol for another 21 hr. Cell lysates were collected for immunoblot analysis using p21^{Cip1} antibody.

(B) P21AS relieved inhibition of Taxol-mediated p34^{Cdc2} activation by p185^{ErbB2}. The 435.eB cells were treated with oligonucleotide in a similar way as in (A), and the cells were cultured in media containing 0.02 μM Taxol for 0 or 8 hr. Activation of p34^{Cdc2} by Taxol and the p34^{Cdc2} protein levels were assayed as in (A).

(C) P21AS sensitized the 435.eB cells to Taxol-induced apoptosis. The 435.eB cells were treated in a similar way as in (A), and the cells were cultured in Taxol-containing (0.02 μM) media for 0, 15, and 21 hr and harvested. Flow cytometry analysis was performed as in Figure 2B.

Overexpression of ErbB2 Does Not Inhibit Taxol-Induced Apoptosis in p21$^{-/-}$ Mouse Embryonic Fibroblasts

To further test the requirment of p21^{Cip1} for p185^{ErbB2} antiapoptotic function, we examined whether p185^{ErbB2} could block Taxol-induced apoptosis in p21^{Cip1} null cells. The ErbB2 expression vector (pCMVerbB2) or control vector (pCMVneo) was transfected into mouse embryonic fibroblasts (MEF) from a p21^{Cip1} knockout mouse (p21$^{-/-}$ MEF) or from a wild-type mouse (wt MEF) (Montes de Oca Luna et al., 1997). Western blot analysis using p185^{ErbB2} antibodies demonstrated overexpression of p185^{ErbB2} in pCMVerbB2-transfected p21$^{-/-}$ MEF and wt MEF compared to controls (Figure 7A). In addition, the overexpressed p185^{ErbB2} in wt MEF has led to a dramatic increase of p21^{Cip1} expression (Figure 7A). However, although overexpression of p185^{ErbB2} in wt MEF conferred resistance to Taxol-induced apoptosis, overexpression of p185^{ErbB2} in p21$^{-/-}$ MEF did not demonstrate a similar antiapoptotic response (Figure 7B). Similar results were

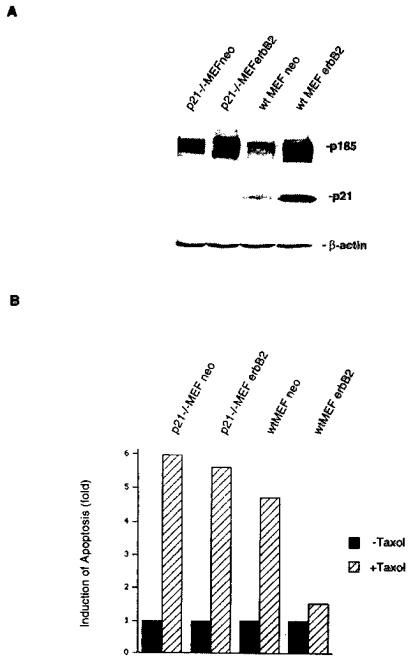

Figure 7. Overexpression of $p185^{ErbB2}$ Cannot Protect $p21^{-/-}$ Mouse Embryonic Fibroblasts from Taxol-Induced Apoptosis

(A) Transfection of pCMVerbB2 led to enhanced expression of $p185^{ErbB2}$ in $p21^{-/-}$ MEF and wt MEF (top), and $p185^{ErbB2}$ upregulated $p21^{Cip1}$ in wt MEF (middle). The $p21^{-/-}$ MEF and wt MEF were transfected with pCMVneo or pCMVerbB2. Forty hours later, protein lysates were extracted for Western blot analyses using anti-$p185^{ErbB2}$, anti-$p21^{Cip1}$, or anti-β-actin antibodies as controls (bottom).

(B) $p185^{ErbB2}$ did not protect $p21^{-/-}$ MEF from Taxol-induced apoptosis. The $p21^{-/-}$ MEF and wt MEF were cultured with (+Taxol) or without (−Taxol) Taxol for an additional 24 hr after transfection with pCMVneo or pCMVerbB2 for 36 hr. Cells were then harvested for double-label flow cytometry analyses. The folds of induction of apoptosis in Taxol-treated samples were calculated by standardization of the percent of apoptotic cells (including cells with high levels of biotin-16-dUTP labeling in G2/M phase as well as sub-G1 apoptotic cells) in these samples over that in the corresponding untreated cells.

obtained when apoptotic cells were quantitated by staining with annexin-specific antibodies (data not shown). These findings provided consistent evidence that $p21^{Cip1}$ participates in the p185-mediated resistance to Taxol-induced apoptosis.

Discussion

Activation of $p34^{Cdc2}$ Is Required for Taxol-Induced Apoptosis

Activation of $p34^{Cdc2}$ kinase is the biochemical step required for mitosis and has been implicated as an important event during chemotherapy-induced apoptosis in certain cancer types (Meikrantz and Schlegel, 1996). Although it was suggested that chromatin condensation and lamina disassembly during apoptosis involve different processes from those operating in mitosis, similar transient activations of $p34^{Cdc2}$ kinase were observed in Taxol-treated apoptotic HeLa cells (Donaldson et al., 1994). In this study, we demonstrated that Taxol induced apoptosis of MDA-MB-435 breast cancer cells at the G2/M phase of the cell cycle through activation of $p34^{Cdc2}$. Activation of $p34^{Cdc2}$–cyclin B1 kinase is required for Taxol-induced apoptosis in breast cancer cells because Taxol-mediated activation of $p34^{Cdc2}$ kinase occurred prior to Taxol-induced apoptosis and because inhibition of Taxol-mediated activation of $p34^{Cdc2}$ kinase by a chemical inhibitor and by the dominant-negative mutant of $p34^{Cdc2}$ diminished Taxol-induced apoptosis.

$p185^{ErbB2}$ Confers Resistance to Taxol-Induced Apoptosis by Inhibiting $p34^{Cdc2}$ Activation

Several growth factors and growth factor receptors have been shown to modulate apoptosis (Rodeck et al., 1997). Here, we have provided direct evidence that overexpression of $p185^{ErbB2}$ in breast cancer cells can confer resistance to Taxol-induced apoptosis. The antiapoptotic effect of $p185^{ErbB2}$ was also observed in $p185^{ErbB2}$-overexpressing MDA-MB-361 and BT-474 breast cancer cell lines (Yu et al., unpublished data) that were established from breast tumors of other patients, indicating that resistance to Taxol-induced apoptosis in $p185^{ErbB2}$-overexpressing breast cancer cells is not limited to a single cell line but is of general importance. Our data indicated that overexpression of $p185^{ErbB2}$ in breast cancer cells conferred resistance to Taxol-induced apoptosis via Bcl-2 independent pathways. Interestingly, overexpression of $p185^{ErbB2}$ in 435.eB transfectants resulted in a reduced activation of $p34^{Cdc2}$ kinase compared to p185-low-expressing 435.neo control cells. Moreover, inhibition of Taxol-mediated activation of $p34^{Cdc2}$ kinase by $p185^{ErbB2}$ corresponded to the delayed cell entrance to G2/M phase after Taxol treatment and paralleled the inhibition of Taxol-induced apoptosis. Therefore, at least one of the mechanisms for $p185^{ErbB2}$ antiapoptotic function is inhibition of Taxol-mediated activation of $p34^{Cdc2}$ kinase.

Upregulation of $p21^{Cip1}$ Contributes to Inhibition of Taxol-Mediated $p34^{Cdc2}$ Activation by $p185^{ErbB2}$

In this study, we found that overexpression of $p185^{ErbB2}$ transcriptionally upregulates the Cdk inhibitor $p21^{Cip1}$ in MDA-MB-435 cells. The $p185^{ErbB2}$-mediated upregulation of $p21^{Cip1}$ is p53 independent, because the MDA-MB-435 cells do not contain the wt *p53* gene (Lesoon-Wood et al., 1995).

$p21^{Cip1}$ was originally believed not to be a universal inhibitor of Cdks but to display selectivity for G1/S phase Cdk–cyclin complexes (e.g., Cdk2) (Harper et al., 1993). Recently, $p21^{Cip1}$ was also demonstrated to contribute to regulation of G2/M transition (Dulic et al., 1998), and Taxol was shown to increase $p21^{Cip1}$ expression, which associated with $p34^{Cdc2}$ (Barboule et al., 1997). We report here that in 435.eB cells, $p185^{ErbB2}$ upregulated $p21^{Cip1}$, which also complexed with $p34^{Cdc2}$. Moreover, we demonstrated that $p21^{Cip1}$ directly inhibited the G2/M phase $p34^{Cdc2}$–cyclin B1 in vitro, although less effectively than it inhibits the G1/S phase Cdk2. The association of $p21^{Cip1}$ with $p34^{Cdc2}$ in 435.eB cells and the ability of $p21^{Cip1}$ to inhibit $p34^{Cdc2}$ activity in vitro suggest that $p21^{Cip1}$ may inhibit $p34^{Cdc2}$ activity in 435.eB cells. This notion is also

supported by our data that $p21^{Cip1}$ antisense oligonucleotide sensitized 435.eB cells to Taxol-mediated activation of $p34^{Cdc2}$. The $p21^{Cip1}$-mediated dual inhibition at G1/S and G2/M phases may protect p185-overexpressing breast cancer cells from Taxol-induced apoptosis: $p21^{Cip1}$ directly inhibits Taxol-mediated activation of $p34^{Cdc2}$, which delays or prevents cell entrance to G2/M phase, resulting in inhibition of apoptosis; or $p21^{Cip1}$ arrests those cells progressing through aberrant mitosis in G1, which indirectly prevents or delays the cells from entering G2/M phase and undergoing apoptosis. Although multiple mechanisms may be involved, inhibition of $p34^{Cdc2}$ by $p21^{Cip1}$ is likely one of the major mechanisms of apoptosis resistance in p185-overexpressing cells, since activation of $p34^{Cdc2}$, but not of Cdk2 or Cdk4, is required for Taxol-induced apoptosis.

Molecular Basis of Taxol-Induced Apoptosis and $p185^{ErbB2}$ Antiapoptosis

Based on previous studies and data presented in this study, we propose a model for Taxol-induced apoptosis and $p185^{ErbB2}$-mediated antiapoptosis in breast cancer cells. Taxol can induce activation of $p34^{Cdc2}$ kinase in MDA-MB-435 breast cancer cells that contributes to the induction of apoptosis at the G2/M phase, whereas overexpression of $p185^{ErbB2}$ in MDA-MB-435 cells (435.eB transfectants) impedes Taxol-induced apoptosis by upregulation of the Cdk inhibitor $p21^{Cip1}$, which in turn inhibits Taxol-mediated activation of $p34^{Cdc2}$. This model synthesized the critical role of the G2/M Cdk $p34^{Cdc2}$ in apoptosis induction, the function of $p21^{Cip1}$ as a mammalian (human breast cancer) cell G2/M Cdk inhibitor, and the effects of overexpression of the receptor tyrosine kinase $p185^{ErbB2}$ on $p21^{Cip1}$ expression into our understanding of the molecular basis of Taxol-induced apoptosis and $p185^{ErbB2}$ antiapoptosis. Furthermore, the model provides a molecular mechanism, although it may not be the only mechanism, that underlies the Taxol-resistance phenomenon in ErbB2-overexpressing breast cancers.

Experimental Procedures

Cell Lines and Culture

The human breast cancer cell line MDA-MB-435, the 435.eB transfectants, their revertants, and control 435.neo cells were obtained, established, and cultured as previously reported (Yu et al., 1996). The $p21^{-/-}$ MEF and wt MEF were from Dr. Guillermina Lozano (The University of Texas, M. D. Anderson Cancer Center).

Antibodies and Reagents

Antibodies were purchased from commercial sources: human $p34^{Cdc2}$, cyclin B1 monoclonal antibodies, and Cdk2 polyclonal antibodies from Santa Cruz Biotechnology, Inc. (Santa Cruz, CA); Bcl-2 antibody from DAKO Corporation (Carpinteria, CA); human $p21^{Cip1}$ polyclonal and $p185^{ErbB2}$ monoclonal antibodies from Oncogene Science, Inc. (Cambridge, MA); and β-actin monoclonal antibody from Sigma (St. Louis, MO). Taxol was purchased from Mead Johnson, Inc. (Princeton, NJ). Recombinant $p34^{Cdc2}$–cyclin B1 was purchased from New England BioLabs, Inc. (Beverly, MA).

Transmission Electron Microscopy

Cells were washed and fixed in 2% glutaraldehyde in 0.2 M sodium cacodylate buffer overnight at 4°C. Cells were postfixed in cacodylate-buffered 1% osmium tetroxide, dehydrated, and embedded in epon. Thin sections were poststained with uranyl acetate and lead citrate and viewed on a JOEL JEM 1200 Ex transmission electron microscope.

DNA Fragmentation Assay

Approximately 1×10^7 cells were incubated on ice in 100 μl of DNA isolation buffer (10 mM Tris, 1 mM EDTA, and 0.2% Triton X-100) for 30 min and then added with 100 μl of PBS. After centrifugation, the low molecular weight DNA was extracted from the supernatant with phenol/chloroform and precipitated with ethanol. Ten micrograms of DNA from each sample was analyzed by 1.8% agarose gel electrophoresis.

Flow Cytometry Analysis

Cells were harvested by trypsinization and fixed in 1% formaldehyde on ice for 20 min and washed once with PBS. For multiparameter flow cytometry analysis, the cells were incubated in terminal deoxynucleotidyl transferase (TdT) solution (0.1 M sodium cacodylate, 1 mM $CoCl_2$, 0.1 mM dithiothreitol, 0.05 mg/ml bovine serum albumin, 10 U TdT, and 0.5 nM biotin-16-dUTP) at 37°C for 30 min, transferred to 100 μl of staining solution (4× SSC, 5% dry milk, 0.1% Triton X-100, and 2.5 ng/μl Avidin-FITC), and incubated in the dark at room temperature for 30 min. Finally, the cells were stained in 500 μl of propidium iodide (PI) solution (0.5 μg/ml of PI and 0.1% RNase A). For single-label flow cytometry analysis, cultured cells were harvested and fixed in a similar manner and then stained in 500 μl of PI solution. Flow cytometry was performed on a FACScan flow cytometer (Becton Dickinson, San Jose, CA). Cell cycle profile was analyzed using MultiCycle software (Phoenix Flow Systems, San Diego, CA), and FITC signal was analyzed using Epics Elite Software (Coulter Corp., Miami, FL).

Immunocomplex-Kinase Assay

Cells (3×10^6) were lysed with the immunoprecipitation (IP) buffer (1% Triton X-100, 150 mM NaCl, 10 mM Tris at pH 7.4, 1 mM ethylene glycol-bis-tetraacetic acid, 0.2 mM sodium vanadate, 0.2 mM phenylmethylsulfonyl fluoride, and 0.5% NP-40). Forty micrograms of protein from each sample was incubated at 4°C for 3 hr with 1 μg of antibodies and for another 3 hr after addition of protein A–agarose. The immunoprecipitates were washed twice with IP buffer and once with kinase buffer (10 mM Tris [pH 7.4], 150 mM NaCl, 10 mM $MgCl_2$, and 0.5 mM DTT) and resuspended in 40 μl kinase buffer containing 1 μg of histone H1, 25 μM of ATP, and 2.5 μCi of γ-^{32}P]ATP. Following 30 min incubation at 30°C, the reaction was terminated by adding 40 μl of 2× SDS sample buffer (125 mM Tris [pH 6.8], 4% SDS, 20% glycerol, 10% 2-mercaptoethanol, and 0.004% bromophenol blue). Samples were resolved on 12% SDS-PAGE and analyzed by autoradiography.

Immunoprecipitation and Immunoblotting

Immunoprecipitation was performed as described in Immunocomplex-Kinase Assay, and immunoblot analyses were performed as described previously (Yu et al., 1990).

Reverse Transcriptase-Polymerase Chain Reaction

Total RNA was isolated using RNAZolB reagent (Tel-Test Inc., Friendswood, TX). Reverse transcription was performed using SuperScript Preamplification System (Life Technologies, Inc., Gaithersburg, MD). Ten percent of the RT products (2 μl) were used for 30 cycles of PCR (94°C 30 s, 56°C 30 s, 72°C 45 s) using GeneAmp System 9600 (Perkin Elmer, Norwalk, CT). The sequence of forward primer for the β-globin gene is GCACGTGGATCCTGAGAACTTCAG (both pCMVcdc2-dn and pCMVcdk2-dn contain this β-globin gene sequence at the 5′ of inserts). The sequence of reverse primers are CGAGCTGACCCCAGCAATACTTCT for Cdc2 and CAGGAGGATTT CAGGAGCTCGGTA for Cdk2, respectively.

Northern Blot Analysis

Twenty micrograms of RNA was denatured with glyoxal buffer, separated by electrophoresis on a 1% agarose gel in 10 mM $NaPO_4$ (pH 6.8) buffer, and blotted onto a nylon membrane. The membrane was hybridized at 65°C with the ^{32}P-labeled *$p21^{Cip1}$* cDNA probe for detection of $p21^{Cip1}$ or with a β-actin cDNA probe as an internal loading control.

Luciferase Assays

MDA-MB-435 cells were cotransfected with pCMV-lacZ and the pWWP-Luc reporter gene with either the pCMVneo control vector or with the pCMVerbB2 expression vector using cationic liposome. Forty hours later, cells were lysed with 500 μl of 1× lysis buffer (Promega, Madison, WI) for 10 min at room temperature. After centrifugation, 100 μl of supernatant was used for a β-gal assay to determine transfection efficiency, and 15–30 μl of supernatant was added to 100 μl of reconstituted luciferase assay reagent in the luciferase assay kit (Promega). Light emission was detected by a luminometer.

Use of GST-p21 for Inhibition of Cdc2–Cyclin B1 Kinase Activity

The GST-p21 fusion protein or GST protein was isolated from BL21 (DE3) bacteria transformed with either pGEX-2T-WAF1-S or pGEX-2T as previously described (El-Deiry et al., 1993). Immunoprecipitates of anti-cyclin B1 or anti-Cdk2 from MDA-MB-435 total cell lysates or recombinant Cdc2–cyclin B1 kinases were incubated at 30°C for 30 min in 20 μl of kinase buffer with 10 μg of GST-p21 or GST protein. Samples were then processed for kinase assay.

Antisense Oligonucleotides

Phosphorothioate oligodeoxynucleotides (5 μg) and cationic liposome, DC-Chol:DOPE (75 nmol) were incubated at 37°C for 15 min. The oligonucleotide–liposome mixture was diluted with serum-free medium and added to the cells for 36 hr. Cells were then treated with or without 0.02 μM Taxol for various times. We used antisense oligonucleotides based on the $p21^{Cip1}$ coding sequence complementary to the region of the initiation codon (p21-AS, 5′-CCCAGCCGGTT CTGACATGGCGCC-3′) and the scrambled $p21^{Cip1}$ antisense oligonucleotides as control (p21-S, 5′-CCGCACGGAGCGCTGCGTTCT ACC-3′). These oligonucleotides were purchased from Genosys Inc. (Woodlands, TX).

Acknowledgments

The authors thank Dr. Wafik S. El-Deiry for the GST-$p21^{Cip1}$ construct; Dr. Guillermina Lozano for $p21^{-/-}$ MEF and wt MEF; Dr. Jeffrey W. Harper for pCMVcdk2-dn and pCMVcdk4-dn; Dr. William Klein, Dr. Daniel Carson, and Ms. Rebecca Grijalva for critical reading of the manuscript; Mr. Dantong Sun for technical assistance; and Ms. Karen Ramirez for flow cytometry analysis. This research was supported by Grants CA60488 from the National Institutes of Health (to D. Y.), DAMD17-98-1-8338 from the United States Army Medical Research and Materiel Command (USAMRMC) (to D. Y.), M. D. Anderson Breast Cancer Research Program Fund (to D. Y.), and predoctoral fellowships from USAMRMC (T. J. and M. T.) and from R. B. Hite foundation (J. Y.)

Received March 2, 1998; revised September 25, 1998.

References

Barboule, N., Chadebech, P., Baldin, V., Vidal, S., and Valette, A. (1997). Involvement of p21 in mitotic exit after paclitaxel treatment in MCF-7 breast adenocarcinoma cell line. Oncogene *15*, 2867–2875.

Blagosklonny, M.V., Schulte, T., Nguyen, P., Trepel, J., and Neckers, L.M. (1996). Taxol-induced apoptosis and phosphorylation of Bcl-2 protein involves c-Raf-1 and represents a novel c-Raf-1 signal transduction pathway. Cancer Res. *56*, 1851–1854.

Coleman, T.R., and Dunphy, W.G. (1994). Cdc2 regulatory factors. Curr. Opin. Cell Biol. *6*, 877–882.

Collins, M.K.L., and Rivas, A.L. (1993). The control of apoptosis in mammalian cells. Trends Biochem. Sci. *18*, 307–309.

Darzynkiewicz, Z., Bruno, S., Del Bino, G., Gorczyca, W., Hotz, M.A., Lassota, P., and Traganos, F. (1992). Features of apoptotic cells measured by flow cytometry. Cytometry *13*, 795–808.

Dickman, S. (1998). Antibodies stage a comeback in cancer treatment. Science *280*, 1196–1197.

Ding, A.H., Porteu, F., Sanchez, E., and Nathan, C.F. (1990). Shared actions of endotoxin and Taxol on TNF receptors and TNF release. Science *248*, 370–372.

Donaldson, K.L., Goolsby, G.L., Kiener, P.A., and Wahl, A.F. (1994). Activation of $p34^{cdc2}$ coincident with Taxol-induced apoptosis. Cell Growth Differ. *5*, 1041–1050.

Draetta, G., Luca, F., Westendorf, J., Brizuela, L., Reuderman, J., and Beach, D. (1989). Cdc2 protein kinase is complexed with both cyclin A and B: evidence for proteolytic inactivation of MPF. Cell *56*, 829–838.

Dulic, V., Stein, G.H., Far, D.F., and Reed, S.I. (1998). Nuclear accumulation of $p21^{cip1}$ at the onset of mitosis: a role at the G2/M-phase transition. Mol. Cell. Biol. *18*, 546–557.

El-Deiry, W., Tokino, T., Velculescu, V.E., Levy, D.B., Parson, R., Trent, J.M., Lin, D., Mercer, W.E., Kinzler, K.W., and Voglestein, B. (1993). Waf1, a potential mediator of p53 tumor suppression. Cell *75*, 817–825.

Fisher, D.E. (1994). Apoptosis in cancer therapy: crossing the threshold. Cell *78*, 539–542.

Guadagno, T.M., and Newport, J.W. (1996). Cdk2 kinase is required for entry into mitosis as a positive regulator of cdc2–cyclin B kinase activity. Cell *84*, 73–83.

Harper, J.W., Adami, G.R., Wei, N., Keyomarsi, K., and Elledege, S.J. (1993). The p21 Cdk-interacting protein Cip1 is a potent inhibitor of G1 cyclin-dependent kinases. Cell *75*, 805–816.

Holmes, F.A., Walters, R.S., Theriault, R.L., Forman, A.D., Newton, L.K., Raber, M.N., Buzdar, A.U., Frye, D.K., and Hortobagyi, G.N. (1991). Phase II trial of Taxol, an active drug in the treatment of metastatic breast cancer. J. Natl. Cancer Inst. *83*, 1797–1805.

Horwitz, S.B. (1992). Mechanism of action of Taxol. Trends Pharmacol. Sci. *13*, 134–136.

Jacks, T., and Weinberg, R.A. (1996). Cell-cycle control and its watchman. Nature *381*, 643–644.

Lesoon-Wood, L.A., Kim, W.H., Kleinman, H.K., Weintraub, B.D., and Mixson, A.J. (1995). Systemic gene therapy with p53 reduces growth and metastases of a malignant human breast cancer in nude mice. Hum. Gene Ther. *6*, 395–405.

Manthey, C.L., Brandes, M.E., Perera, P.Y., and Vogel, S.N. (1992). Taxol increases steady-state levels of lipopolysaccharide-inducible genes and protein-tyrosine phosphorylation in murine macrophages. J. Immunol. *149*, 2459–2465.

Meikrantz, W., and Schlegel, R. (1996). Suppression of apoptosis by dominant negative mutants of cyclin-dependent protein kinases. J. Biol. Chem. *271*, 10205–10209.

Montes de Oca Luna, R., Amelse, L.L., Chavez-Reyes, A., Evans, S.C., Brugarolas, J., Jacks, T., and Lozano, G. (1997). Deletion of p21 cannot substitute for p53 loss in rescue of mdm2 null lethality. Nat. Genet. *16*, 336–337.

Niculescu, A.B.I., Chen, X., Smeets, M., Hengst, L., Prives, C., and Reed, S.I. (1998). Effects of $p21^{Cip1/Waf1}$ at both the G_1/S and the G_2/M cell cycle transitions: pRb is a critical determinant in blocking DNA replication and in preventing endoreduplication. Mol. Cell. Biol. *18*, 629–643.

Rodeck, U., Jost, M., Kari, C., Shih, D.T., Lavker, R.M., Ewert, D.L., and Jensen, P.J. (1997). EGF-R dependent regulation of keratinocyte survival. J. Cell Sci. *110*, 113–121.

Slamon, D.J., Clark, G.M., Wong, S.G., Levin, W.J., Ullrich, A., and McGuire, W.L. (1987). Human breast cancer: correlation of relapse and survival with amplification of the HER-2/*neu* oncogene. Science *235*, 177–182.

van den Heuvel, S., and Harlow, E. (1993). Distinct roles for cyclin-dependent kinases in cell cycle control. Science *262*, 2050–2054.

Vesely, J., Havlicek, L., Strnad, M., Blow, J.J., Donella-Deana, A., Pinna, L., Letham, D.S., Kato, J.Y., Detivaud, L., Leclerc, S., and Meijer, L. (1994). Inhibition of cyclin-dependent kinases by purine analogues. Eur. J. Biochem. *224*, 771–786.

Wahl, A.F., Donaldson, K.L., Fairchild, C., Lee, F.Y.F., Foster, S.A., Demers, G.W., and Galloway, D.A. (1996). Loss of normal p53 function confers sensitization to Taxol by increasing G2/M arrest and apoptosis. Nat. Med. *2*, 72–79.

Waldman, T., Lengauer, C., Kinzler, K.W., and Vogelstein, B. (1996). Uncoupling of S phase and mitosis induced by anticancer agents in cells lacking p21. Nature *381*, 713–716.

Yu, D., Suen, T.-C., Yan, D.-H., Chang, L.S., and Hung, M.-C. (1990). Transcriptional repression of the *neu* protooncogene by the adenovirus 5 E1A gene products. Proc. Natl. Acad. Sci. USA *87*, 4499–4503.

Yu, D., Liu, B., Tan, M., Li, J., Wang, S.-S., and Hung, M.-C. (1996). Overexpression of c-erbB-2/neu in breast cancer cells confers increased resistance to Taxol via mdr-1-independent mechanisms. Oncogene *13*, 1359–1365.